

**Th-AM-Sym-1 PHOTOTRANSDUCTION IN RODS AND CONES: AN OVERVIEW.** K.-W. Yau, Howard Hughes Medical Institute and Department of Neuroscience, Johns Hopkins University School of Medicine.

Retinal rods and cones respond to light with a membrane hyperpolarization, generated by the closure of a cyclic GMP-gated channel which in darkness lets  $\text{Na}^+$  and  $\text{Ca}^{++}$  into the cells' outer segments. In rods, phototransduction is known to involve the following reaction cascade: photoisomerized rhodopsin  $\rightarrow$  G-protein activation  $\rightarrow$  cyclic GMP phosphodiesterase stimulation  $\rightarrow$  cyclic GMP hydrolysis  $\rightarrow$  conductance closure. The latest evidence suggests that a similar cascade most probably functions in cones. As a result of the conductance closure, the  $\text{Ca}^{++}$  influx stops and the consequent imbalance between influx and efflux causes a decrease in the intracellular concentration of  $\text{Ca}^{++}$  in the light. This decrease in  $\text{Ca}^{++}$  exerts a negative-feedback regulation on the phototransduction cascade, and leads to light adaptation in the receptors. When this  $\text{Ca}^{++}$  feedback was experimentally removed by preventing the internal  $\text{Ca}^{++}$  from declining during illumination, no active adaptation to light was observed in either rods or cones. As might be expected, the speed of the  $\text{Ca}^{++}$  decline (and hence the feedback) seems to be matched to the kinetics of phototransduction so that the two can function in unison; in cones, where the latter is more rapid, the speed of  $\text{Ca}^{++}$  decline is also faster. It is still unclear why cones are much less sensitive to light than rods, though this does not appear to be just due to a quantitative difference in the effect of  $\text{Ca}^{++}$  feedback between the two types of receptors. The distinct surface geometries of the outer segments in rods and cones have long been a curiosity. We think, however, that the cone surface geometry serves simply to allow the regenerated chromophore from the cell exterior to gain rapid access to the bleached visual pigment under bright light conditions.

**Th-AM-Sym-2 INTRACELLULAR BIOCHEMICAL MANIPULATION OF PHOTOTRANSDUCTION IN DETACHED ROD OUTER SEGMENTS.** P.B. Detwiler, G. Rispoli, W.A. Sather & Eric A. Ertel. Univ. of Washington, Dept. Physiol. & Biophys., Seattle, WA.

The strict division of labor in vertebrate photoreceptors is aided in part by distinct regional differences in morphology. Phototransduction is performed solely in the outer segment whereas chores related to the biochemical maintenance of the cell and synaptic transmission are performed in the inner segment and synaptic terminal. The intact rod outer segment can be detached from the rest of the photoreceptor and the function of the phototransduction machinery it contains can be restored and studied in isolation using whole-cell recording and intracellular dialysis to alter the biochemical composition of outer segment cytoplasm <sup>1</sup>.

In whole-cell voltage clamp ( $V_H = -29$  mV) detached outer segments from Gekko rods developed and maintained a stable light-sensitive inward dark current when dialyzed with a standard pipet filling solution that has been supplemented with nucleotides but not when dialyzed with unsupplemented solution. The amplitude of inward current increases with [cGMP] and thus is sensitive to changes in phosphodiesterase (PDE) activity. Manipulation of critical nucleotides influences the development and light sensitivity of the dark current as expected if light-evoked changes in PDE activity were controlled by a G protein mediated transduction cascade <sup>2</sup>.

Rod outer segments dialyzed with solutions containing ATP and GTP use endogenous guanylate cyclase to synthesize cGMP and generate dark current. Reduction in external Ca causes an initial small rapid increase in dark current followed by a delayed larger and slower increase. The initial increase is due to a direct effect of low external Ca on the conductance of the light-regulated channel. The channel can be modified; its sensitivity to Ca block is reduced by the combined effects of cGMP and nucleoside triphosphate. The amplitude of the delayed increase in dark current increases with [GTP] in the dialysis solution and is reduced by imidodiphosphate, a guanylate cyclase inhibitor <sup>3</sup>. We conclude that the slow component of the 0 Ca response is due to stimulation of G. cyclase by reduced internal Ca <sup>4</sup>. The Ca regulation of G cyclase plays an important role in the recovery phase of the light response and can account for some but not all the changes associated with light adaptation. References: 1. Sather & Detwiler, Soc. Neurosci. Abstr. 12:629, 1986; 2. Sather & Detwiler, PNAS 84:9290, 1987; 3. P. Robinson & R. Cote, personal communication; 4. Rispoli, Sather & Detwiler, Biophys. J. 53:388a, 1988.

**Th-AM-Sym-3 ROLE OF  $\text{Ca}^{2+}$  IN THE LIGHT RESPONSE OF VERTEBRATE PHOTORECEPTORS** P.A. McNaughton. Physiological Laboratory, University of Cambridge, Cambridge CB2 3EG, UK.

Two main topics will be discussed: the means by which the intracellular calcium level in photoreceptors is regulated, and the role of intracellular  $\text{Ca}^{2+}$  in the light response.

**Control of  $[\text{Ca}^{2+}]_i$ .** Approximately 10% of the light-sensitive current in salamander rods is carried by  $\text{Ca}^{2+}$ , this being the only significant route for  $\text{Ca}^{2+}$  entry into the outer segment. Calcium is extruded across the outer segment membrane by an exchange mechanism whose stoichiometry is  $4\text{Na}^+ : 1\text{Ca}^{2+}$ ,  $1\text{K}^+$ , which would be capable of supporting calcium extrusion down to levels as low as  $[\text{Ca}^{2+}]_i = 2 \times 10^{-10} \text{M}$  (see Cervetto et al, this meeting). The forward mode of the exchange is activated by  $[\text{Ca}^{2+}]_i$  in a first-order manner with a mean  $K_M$  of  $1.6 \mu\text{M}$ . External  $\text{Na}^+$  activates the exchange in a sigmoidal manner, with half-activation at  $[\text{Na}^+]_o = 93 \text{mM}$  in the absence of other competing ions and with  $V_M = -14 \text{mV}$ . The forward exchange rate is reduced e-fold by a 70mV depolarization, apparently because the binding of external  $\text{Na}^+$  is voltage-sensitive. Inside the outer segment  $\text{Ca}^{2+}$  is rapidly and reversibly buffered by two systems: a saturable high-affinity buffer, and a low-affinity buffer which maintains a bound:free ratio of about 16:1. Free  $[\text{Ca}^{2+}]_i$  measured with aequorin is  $0.4 \mu\text{M}$  in darkness, and falls to a level below  $0.3 \mu\text{M}$  with a mean time constant of 0.7sec.

**Role of  $\text{Ca}^{2+}$  in the light response.** Calcium inhibits the guanylate cyclase responsible for producing cGMP from GTP, and simulations using a model system show that this inhibition can account for the suppression of current in low  $[\text{Na}^+]_o$ , for the increase of current in low  $[\text{Ca}^{2+}]_o$ , and for the adaptation caused by a background light.

**Th-AM-Sym-4** THE cGMP-GATED CHANNEL OF MAMMALIAN ROD PHOTORECEPTORS: MOLECULAR STRUCTURE AND ELECTRICAL PROPERTIES. U.B. Kaupp, Institut für Biologische Informationsverarbeitung, Kernforschungsanlage Jülich, D-5170 Jülich, FRG

Cyclic GMP controls the opening of *light-regulated* channels in the plasma membrane, probably by binding to a specific receptor site on the channel protein. We identified, purified and functionally reconstituted the cGMP-gated channel protein from mammalian rod photoreceptors. The functional channel in the membrane probably exists as a *homotetramer* or *pentamer* which is composed of 4 or 5 identical or similar 63 kD subunits. The reconstituted channel is cooperatively activated by at least 3, possibly more, cGMP molecules with an  $EC_{50}$  value between 10 and 30  $\mu$ M. The macroscopic electrical properties of the channel were studied *in situ* in excised membrane patches from bovine rod outer segments, and single channel parameters were investigated after insertion of the purified protein into planar lipid bilayer. I will discuss the mechanism of channel activation by cGMP, its ion selectivity, and the control and permeation of the channel by divalent cations.

The amino acid sequence of the 63 kD polypeptide has been deduced from channel specific cDNA. Several features of the primary structure of the cGMP-gated channel will be compared with channel-forming or otherwise related proteins.

**Th-AM-Sym-5** LOCALIZATION AND STRUCTURAL ORGANIZATION OF THE cGMP-DEPENDENT CHANNEL OF RETINAL ROD PHOTORECEPTOR CELLS. R.S. Molday, Department of Biochemistry, University of British Columbia, Vancouver, B.C. V6T 1W5, Canada.

The rod outer segment (ROS) of vertebrate photoreceptor cells consists of hundreds of stacked disks surrounded by a plasma membrane. In order to study the molecular composition and function of these membranes, we have developed a ricin affinity density perturbation method to separate the plasma membrane from disk membranes. The plasma membrane which contains many unique proteins was used for the production of monoclonal antibodies. One antibody designated PMc 1D1 was found to bind to a 63kD protein of ROS membranes and the purified cGMP-dependent cation channel of ROS (Cook et al., PNAS 84, 585, 1987). Western blotting analysis and immunogold labeling for electron microscopy indicated that the 63kD channel is a major protein of ROS plasma membranes, but is not detectable in disk membranes. Functional reconstitution studies also have indicated that the cGMP-dependent channel activity is localized only in the plasma membrane at a density of about 300 channels per  $\mu$ m<sup>2</sup>. The PMc 1D1 antibody has been used to immunoprecipitate the 63kD protein and channel activity. A 240kD protein reported to copurify with the channel is also immunoprecipitated with this antibody. This protein appears to be a spectrin-like protein which is tightly associated with the channel and may comprise part of the cytoskeletal system of ROS.

**Th-AM-Min-1** EUKARYOTIC INITIATION FACTOR-RNA INTERACTIONS; EQUILIBRIA AND KINETICS. Dixie J. Goss, Chemistry Department, Hunter College CUNY, New York, NY 10021.

The interaction of protein synthesis initiation factors with mRNA is an important step in the initiation of translation. This process includes recognition of a unique structural feature (a "cap") at the 5' terminus of mRNA consisting of 7-methylguanosine in a 5' to 5' linkage via a triphosphate bridge to the first coded base of the mRNA. We have investigated the binding of initiation factors eIF-4F and eIF-4E to cap region analogs (m<sup>7</sup>GpppA, benzyl<sup>7</sup>G and m<sup>2,7</sup>G) to determine the relative affinities and effects on the cap conformation. Both circular dichroism and fluorescence studies of the cap analog m<sup>7</sup>GpppA indicate the two bases occur mainly in the stacked conformation at pH 7.5. Both eIF-4F and eIF-4E caused an increased fluorescence intensity of the m<sup>7</sup>G suggesting that the cap was altered from a stacked to an unstacked conformation. Fluorescence studies also suggest both eIF-4F and eIF-4E preferentially bind the unprotonated (enolate) form of m<sup>7</sup>G. Binding of eIF-4E to cap analogs is a relatively stable interaction with a K<sub>eq</sub> on the order of 10<sup>6</sup>M.

A second important interaction is the association of initiation factor 3 with ribosomal RNA. This interaction is characterized by fast association rates, low activation energy, a decrease in binding with increasing monovalent cation concentration, and small positive values for  $\Delta H$  and  $\Delta S$ . These data suggest mainly electrostatic interactions are involved in association.

Grant Support: AHA-NYC Affil., NSF 86007070, PSC-CUNY Research Award.

**Th-AM-Min-2** RECOGNITION OF RNA STRUCTURES BY RIBOSOMAL PROTEINS David E. Draper, Careen K. Tang, & Jailaxmi V. Vartikar, Department of Chemistry, Johns Hopkins University, Baltimore, MD 21218

The *E. coli* ribosomal protein S4 is a primary initiator of 30S subunit assembly, binding directly to a large domain of the 16S rRNA. It is also a translational repressor, recognizing a specific site on the messenger RNA which encodes it and several other ribosomal proteins (the  $\alpha$  operon). Over the last several years, we have been defining the specific RNA features recognized by S4, and the foldings of the two RNA recognition sites. In the ribosomal RNA, the smallest fragment binding with the same affinity as intact 16S rRNA is still 460 nt (out of 1542). Some hairpins within this fragment can be deleted without affecting binding. It appears that the evolutionarily *variable* regions within this domain are required for proper RNA folding and protein binding. The mRNA regulatory site has been limited to a 139 nt fragment with about the same S4 affinity as the 16S rRNA. Binding measurements with a large collection of site-directed mutations has shown that the RNA has an unusual 'double pseudoknot' structure encompassing the ribosome binding site. In both binding sites we find that protein binding is capable of perturbing the RNA structure significantly. We expect to see some similarity between the two RNAs, but find little, if any, at the level of secondary structure. However, in both RNAs S4 recognition requires an AUA sequence in an exposed loop. It is possible that the two RNAs fold into very different overall structures, but still contain an array of protein contact sites in the same three dimensional configuration.

**Th-AM-Min-3** TRANSCRIPTION TERMINATION FACTOR RHO OF *E. COLI* MOVES ALONG RNA.

Johannes Geiselman, Thomas D. Yager, Stanley C. Gill, James A. McSwiggen and Peter H. von Hippel. Institute of Molecular Biology, University of Oregon, Eugene, OR 97403.

Transcript termination brought about by the rho protein involves the binding of rho to the nascent RNA and the hydrolysis of ATP. These processes lead to the release of the RNA from the ternary transcription complex. We have investigated the physical biochemical properties of rho protein and its interaction with its cofactors, RNA and ATP, in order to build a model of the molecular mechanism of this reaction.

The active form of rho is a hexamer of six identical 46kD protomers. The arrangement of the subunits within the hexamer is not C<sub>6</sub> symmetric, but probably involves D<sub>3</sub> symmetry. There are six ATP binding sites per hexamer. The interaction with ATP can be described by two binding constants per hexamer, corresponding to three strong sites and three sites with a 10-fold lower affinity for ATP. The size of the RNA binding site is 78 nucleotide residues per hexamer, corresponding to 13 nucleotides per rho monomer. However the binding of short RNA oligomers (e.g. oligo(rC)<sub>13</sub>) saturates at three oligomers per rho hexamer (in the concentration range investigated). It appears that the RNA binding site on rho protomers is rather extended, and that each additional nucleotide residue contributes to the binding free energy.

The combination of these and other data suggest a molecular mechanism of transcription termination that predicts a directional movement of rho along the RNA. The model assumes only the existence of an RNA binding site and an ATP binding site on each protomer together with an allosteric interaction between protomers at the dimer level, which in our model represents the functional unit of rho. The same interactions that are responsible for directional movement of rho along RNA are also responsible for transcript release.

**Th-AM-Min-4** STRUCTURE AND FUNCTION OF RIBONUCLEASE P, A CATALYTIC RNA.

Norman R. Pace and David S. Waugh. Department of Biology, Indiana University, Bloomington, IN 47405

The mature 5' ends of tRNAs are generated by the endonuclease RNase P. In *Bacillus subtilis* and *Escherichia coli* RNase P is composed of protein (ca. 14kD) and RNA (ca. 400 nucleotides) elements. *In vitro*, however, the function of the RNase P protein can be supplanted by high salt concentrations. Under these conditions RNase P RNA is an efficient and accurate catalyst.

The secondary structures of the *B. subtilis* and *E. coli* RNase P RNAs are being elucidated using a phylogenetic comparative approach to test base pairing possibilities. A common core of conserved sequence and structure has been identified. Variability among the RNase P RNA sequences is substantially due to the presence or absence of discrete blocks of nucleotides (structural domains) at different locations in the common core.

Because it is present in all the eubacterial RNase P RNAs so far inspected, it seemed likely that the conserved core structure contains the catalytic elements. In order to test this, as well as to obtain a model RNase P RNA that is simpler than the natural forms, we have designed and synthesized an abbreviated RNase P RNA that incorporates only the phylogenetically-defined core elements. Synthetic oligodeoxyribonucleotides incorporating these sequences were assembled in a T7 promoter-containing vector, and the abbreviated (263 nucleotides) RNase P RNA was produced by transcription *in vitro*. The resultant RNA is catalytically active at high salt concentrations. The designed RNA requires higher salt concentrations for optimal activity than do the natural RNase P RNAs, however, its catalytic activity is comparable to the natural forms. The kinetic properties of the artificial RNase P RNA are under study and will be compared to the native form.

**Th-AM-Min-5** PROTEIN-RNA INTERACTIONS IN AN ICOSAHERAL VIRUS. C.V. Stauffacher, Z.G. Chen, Y. Li,

T.S. Schmidt, B. Wu, G. Kamer, \*M. Shanks, \*G. Lomonosoff and J.E. Johnson, Dept. of Biol. Sciences, Purdue Univ., W. Lafayette, IN 47907 and \*John Innes Inst., Norwich NR4 7UH England

Comoviruses are a group of positive strand RNA plant viruses which share many physical and biological properties with the mammalian picornaviruses, such as rhinovirus and poliovirus. The comoviruses are icosahedral viruses with T=1 symmetry, containing sixty copies each of two polypeptides, 42kD and 24kD in molecular weight. The two single strand RNA molecules of the comovirus genome (~3500 and 5900 bases) are separately encapsulated in identical protein shells. The crystallographic structure of two comoviruses, cowpea mosaic virus (CPMV) and beanpod mottle virus (BPMV) have been solved to 3 Å resolution. The 3 Å map of the BPMV capsid containing the small RNA contained a remarkable discovery - icosahedrally ordered RNA in the viral interior. Fully ordered ribonucleotides which correspond to 10% of the RNA molecule are found in a shallow pocket between the two β barrel domains of the large subunit of the capsid. Another set of partially ordered ribonucleotides connects these segments, forming a structure which loops around the icosahedral three fold axis. A total of 18% of the RNA is visible in the electron density map. The structure of the well ordered part of the RNA roughly corresponds to that of a single strand of an A type helix, but with 8 stacked bases per turn and a 3.5Å rise per residue. Close van der Waals contacts between the RNA and the inner surface of the large capsid protein form most of the interaction, with many polar groups extended towards the RNA. Direct hydrogen bonds between the RNA and the protein appear to be limited. The structures of the empty capsid and the capsids with both RNAs show differences which may contain clues about the nature of viral assembly.

**Th-AM-Min-6** STRUCTURE AND RNA BINDING BY THE AVIAN RETROVIRAL NUCLEOCAPSID PROTEIN. Joyce E. Jentoft, Lisa M. Smith, and Josephine Secnik, Department of Biochemistry, Case Western Reserve University, Cleveland, OH 44106

Retroviral nucleocapsid (NC) proteins are small, basic, single-stranded nucleic acid binding proteins that are presumed to function in a histone-like manner in packaging genomic RNA within virions. Despite presumed functional similarity, the only similarity observed in sequences of NC proteins from different classes of retroviruses is the presence of one or two 14 residue cys-his motifs similar to the "zinc finger" motif of transcription factors. One segment of our investigations has focused on the structural/functional role of these regions. We have established that the regions are not "zinc fingers" and that zinc has no effect on NC structure or function. However, we have identified additional motifs within the cys-his regions that may relate to function. Characteristics of the tyrosines, histidines and cysteines comprising 10 of the 28 residues in the two cys-his regions of the avian NC protein have been deduced from <sup>1</sup>H NMR and chemical modification studies. The tyrosines and histidines have properties consistent with largely solvent exposed residues while only one of the cysteines is fully solvent exposed. Two of the remaining cysteines are partially exposed, one is completely buried, and two are in a disulfide bridge. The identity of the four types of cysteine residues will be discussed. These results will be incorporated into a view of the folded structure of this protein. A second segment of our investigation has focused on the nucleic acid binding properties of the NC protein, using <sup>1</sup>H NMR and fluorescence techniques. The current state of characterization of NC complexes with oligo- and polynucleotides will be presented. (Supported by NIH grant GM36948).

## Th-AM-A1

## WITHDRAWN

**Th-AM-A2 CARDIAC DELAYED RECTIFIER K CURRENT RUNDOWN DURING WHOLE CELL DIALYSIS PREVENTED BY DIBUTYRYL cAMP AND ATP.** K. Chinn, Searle Cardiovascular Drug Research, Skokie, IL 60077.

A problem involved in the study of delayed rectifier K currents in cardiac myocytes using the whole cell patch clamp technique is current "rundown". This is the progressive decrease in K current amplitude assayed using fixed voltage pulses. The present investigation examined the utility of adding factors required for cAMP-mediated phosphorylation in reversing rundown. Whole-cell recordings were made at 21°C using electrodes having resistances of 1 - 2 MΩ. K currents were assayed by examining the peak amplitude of the tail current recorded after return to a holding potential of -40 mV from a depolarizing voltage step to +30 mV. K currents began to run down within 15 min after starting recordings, usually decreasing 25 - 100%. Following this, bath application of 1 mM dibutyryl cAMP (dbcAMP), a hydrolysis resistant cAMP analog, increased the size of K currents. In 4 of 5 cells tested, the new K current amplitude was maintained over a period of 15 - 20 min. In 1 cell however, after the initial increase, K current rundown resumed within 5 min. Similar experiments were done after 5 mM ATP was added to the internal (patch pipette) solution. K current rundown in the presence of ATP was similar to that in its absence. However, in the presence of ATP, after addition of 1 mM dbcAMP in all 7 cells tested, the K current was maintained for > 15 min. and progressive K current decay did not resume until after this. The experiments indicate that a combination of both dbcAMP and ATP can prevent rundown by dialysis during whole cell clamp experiments with low resistance electrodes.

**Th-AM-A3 ENHANCEMENT OF ATP-SENSITIVE K CHANNEL ACTIVITY IN HEART CELLS BY PINACIDIL**

J.P. Arena and R.S. Kass, Department of Physiology, University of Rochester Medical Center, Rochester, NY 14642.

Pinacidil is an organic compound that has been shown to enhance a potassium-sensitive outward current in enzymatically isolated guinea pig ventricular cells but the identity of the drug-modified channel has not been established (*Biophys. J.* 53:461a, 1988). In the present set of experiments, we have combined whole cell and single channel measurements of K channel currents in enzymatically-isolated guinea pig ventricular cells with pharmacological probes to determine the target of this novel drug. In whole cell experiments internal electrode solutions contained 5 mM ATP and 11 mM EGTA. External Na was replaced with TRIS and nisoldipine (300 nM) was included to inhibit L-type calcium channel activity. Current was measured in response to voltage pulses applied from -40 mV in the absence and presence of pinacidil (50-100 μM). In single channel experiments pipette and bath solutions contained 140 mM K-aspartate. In pharmacological experiments we found that TEA (20 mM) completely blocked pinacidil-sensitive current but had minimum effects on the inward and delayed rectifier currents. In another set of experiments, we found that the sulphonylurea compound glibenclamide (100 nM) completely inhibited pinacidil-sensitive current with no actions on delayed and inward rectifier currents at 100-fold higher concentrations. These results make it unlikely that the pinacidil-sensitive current is carried via either delayed or inward rectifier K channels. However, because others have shown that glibenclamide potently and specifically blocks the ATP-sensitive K channel in pancreatic islet cells (*J. Biol. Chem.* 262:15840, 1987), our results strongly suggest that the target for pinacidil is the ATP-sensitive potassium channel. Single channel studies confirm this view.

**Th-AM-A4 MODULATION OF POTASSIUM CHANNEL INACTIVATION IN SQUID AXONS BY ATP.** John R. Clay<sup>+</sup> and Ete Z. Szuts<sup>+</sup>. (Intr. by W.J. Adelman, Jr). <sup>+</sup>NINCDS, NIH, Bethesda, MD 20892 and <sup>+</sup>Marine Biological Laboratory, Woods Hole, MA 02543.

We studied the effects of ATP on the delayed rectifier potassium current,  $I_K$ , using standard internal perfusion and voltage clamp techniques. The internal perfusate contained 250 mM K Glutamate, 25 mM  $K_2HPO_4$ , and 400 mM sucrose to which 5 mM  $ATP/Mg^{+2}$  was added. The pH of both the control and test solutions was adjusted to 7.2. The external solution was filtered seawater with  $10^{-6}$  M TTX.  $T = 12^\circ C$ . The voltage clamp protocol consisted of 20 msec depolarizing steps to -20, 0, 20, or 40 mV from a holding potential,  $V_H$ , of -90, -80, ..., or -30 mV. No effect of ATP was observed with  $V_H \leq -80$  mV or with  $V_H = -30$  mV. A significant reduction of  $I_K$  occurred for  $-70 \leq V_H \leq -40$  mV. For example, ATP produced a 25% reduction of  $I_K$  with  $V_H = -60$  mV, and a 65% reduction of  $I_K$  with  $V_H = -50$  mV. The activation kinetics were unaltered. Thus, under our conditions, the net effect of ATP is consistent with a 10-15 mV shift of the inactivation curve for  $I_K$  along the voltage axis. We obtained similar results with  $ATP-\gamma S$  and, surprisingly, with  $ADP/Mg^{+2}$ . However, ADP had no effect when phosphate was replaced with citrate in the perfusate. We attribute the effect of  $ADP+P_i$  to ATP that was synthesized *de novo* by the axon. To test this possibility, we preferentially labeled axonal, but not glial proteins, by incubating axons with internal perfusate which contained either  $[ \gamma^{32}P ]ATP$  or  $ADP+[^{32}P]PO_4$ . Solubilized proteins were analyzed by standard SDS-PAGE and autoradiography. Both incubating conditions caused the phosphorylation of the same polypeptides, which are predominantly above 50 kDa. Thus, the biochemical results are consistent with our interpretation of the electrophysiologically observed effect of  $ADP+P_i$ .

**Th-AM-A5 ATP MODULATION OF THE K CURRENT IN SQUID GIANT AXON: A SINGLE CHANNEL STUDY.**

C. Vandenberg, E. Perozo and F. Bezanilla, Dept. of Physiology, UCLA, Los Angeles, CA 90024 and MBL, Woods Hole, MA 02543.

The macroscopic K conductance in squid axons is increased by phosphorylation, with a slowdown of the turn-on kinetics (PNAS 83:2743, 1986; Biophys. J. 49:215a 1986). Patch clamp experiments were performed to study the single-channel characteristics of the different K channels that form the delayed rectifier current, using illumination of caged ATP to promote channel phosphorylation. Of the two predominant channels (20 pS and 40 pS), the 40 pS channel was specifically modified.

The effectiveness of caged ATP was tested using the dialyzed axon under voltage-clamp conditions. One hour of dialysis with 1 mM caged ATP caused a decrease in the current elicited by voltage pulses to 0 mV from a holding potential of -70 mV, consistent with the inability of caged ATP to support phosphorylation. Illumination of the whole axon liberated ATP and caused an increase in current. Half stimulation of the current was produced in 11 min at  $10^\circ C$  and 2 min at  $20^\circ C$ .

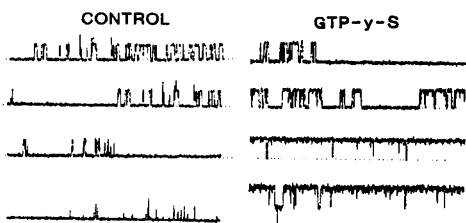
Single K channels were recorded with patch pipettes sealed to the intracellular surface using the cut-open axon technique. ATP was present in the patch pipette as the inactive form of caged ATP, and transformation was achieved by illuminating the tip of the pipette with light of 310-380 nm. The internal solution contained (in mM) 310 K, 4 Mg, 1 caged ATP and 0.5  $\mu M$  catalytic subunit of protein kinase A. The dephosphorylated form of the channels was achieved either by predialyzing the whole axon with 0 ATP solution before cutting it open, or by preincubating the cut-open axon in 0 ATP, 0  $Ca^{2+}$ , 0  $Mg^{2+}$ , 0  $Cl^-$  solution before removing axoplasm. When dephosphorylating conditions were used, the steady-state open probability of the 40 pS channel was very low ( $P_{open} \approx .0005$  at 50 mV), and the channel appeared as a series of infrequent, short-duration events. Upon illumination (and ATP formation), the channel activity increased  $\sim 100$  fold ( $P_{open} \approx .05$  at 50 mV), with no change in the single-channel current amplitude. The effect appeared with a delay of 0.5-10 min following the onset of illumination. When axons were cut open in solutions containing ATP, channel openings were frequent, consistent with the view that this gating mode is associated with the phosphorylated form of the channel. (Supported by USPHS GM 30376 and MDA grants. We thank I. Levitan for catalytic subunit.)

**Th-AM-A6 COUPLING BETWEEN THE G PROTEIN  $G_i$  AND ATRIAL  $K^+$  CHANNELS STUDIED BY A CONCENTRATION JUMP METHOD.** K. Okabe, A. Yatani and A.M. Brown. Department of Physiology and Molecular Biophysics, Baylor College of Medicine, One Baylor Plaza, Houston, TX 77030.

We have shown that the  $\alpha$  subunit of  $G_i$  directly activates atrial muscarinic  $K^+$  channels, ( $K^+[G_i]$ ). To study the kinetics of  $G_i$  protein coupling to these channels we used the concentration-clamp method (Akaike et al., J. Physiol. 379, 1986) on single atrial myocytes of guinea pigs. The myocytes were studied with whole-cell and excised inside-out patch clamp methods during continuous recording and the concentration jumps occurred within 10 ms. Carbachol (Carb) activated whole-cell  $K^+[G_i]$  currents after a delay and both the delay and the time course of activation were reduced at higher concentrations. Carb at  $10^{-6}$  M produced about half-maximal activation and the currents appeared after a latency of  $70 \pm 35$  ms and had an activation half-time of  $655 \pm 112$  ms ( $m \pm s.d.$ ;  $n=8$ ). Jumps in bath concentration of GTP ( $[GTP]$ ) from 0 to 10  $\mu M$  were applied to inside-out patches containing 3-6  $K^+[G_i]$  channels which were previously activated in the cell-attached mode with Carb at  $10^{-6}$  to  $10^{-5}$  M in the pipette. The latency was  $442 \pm 90$  ms and the activation half time was  $800 \pm 230$  ms ( $n=10$ ). Both the latency and the rate of activation decreased linearly with higher  $[GTP]$  and GDP shifted both curves to higher  $[GTP]$ s. In contrast the rate at which the current subsided following a sudden reduction in  $[GTP]$  was independent of  $[GTP]$  or the GTP/GDP ratio and had a half time of about 5 sec. These latencies and washouts are between 4 and 200 times faster than comparable values for coupling between the G protein  $G_i$  and adenylyl cyclase (Gilman, Ann. Rev. Biochem. 56, 1987). Thus either  $G_i$  has a faster GTP:GDP<sup>s</sup> cycle than  $G_s$  or the G protein effector strongly influences G protein kinetics. (Supported by HL36930).

**Th-AM-A7 RECONSTITUTION OF THE ATP-SENSITIVE POTASSIUM CHANNEL OF SKELETAL MUSCLE. ACTIVATION BY A G-PROTEIN DEPENDENT PROCESS.** L. Parent and R. Coronado. Department of Physiology, Baylor College of Medicine. Houston, TX 77030.

K channels inhibited by ATP, K(ATP), were found in the transverse tubular membrane of rabbit skeletal muscle and studied using the planar bilayer recording technique. The K(ATP) channel i) has a conductance of 67 pS (SD=2, n=59) in 260 mM internal, 60 mM external KCl and rectifies weakly at holding potentials more positive than 50 mV; ii) is not activated by internal  $\text{Ca}^{2+}$  or membrane depolarization; and iii) is inhibited by (1-5 mM) internal ATP. Internal  $\text{Mg}^{2+}$  or  $\text{Ca}^{2+}$  decreased outward  $\text{K}^+$  current by a mechanism of block by fast flickering. Activity of K(ATP), measured as open channel probability as a function of time, decreases continuously within 3 min (SD=2, n=22) after a recording is initiated. In presence of cis (internal) 1 mM  $\text{Mg}^{2+}$  and 100  $\mu\text{M}$  GTP- $\gamma$ -S, channel activity is high and persists 120 min (SD=30 min, n=16). Incubation of purified t-tubule vesicles with mM  $\text{AlF}_4$  increases the activity of K(ATP) channels and essentially eliminates channel run-down, mimicking the effect of GTP- $\gamma$ -S. These observations suggest that a nucleotide-binding G-protein regulates ATP-sensitive  $\text{K}^+$  channels in the t-tubule membrane of rabbit skeletal muscle. L. Parent was supported by a post-doctoral fellowship from the Medical Research Council of Canada.



**Th-AM-A8 ATP MEDIATED K-CHANNEL PHOSPHORYLATION IN SQUID AXON IS FURTHER POTENTIATED IN THE PRESENCE OF GTP- $\gamma$ -S.**

E. Perozo and F. Bezanilla Department of Physiology. UCLA School of Medicine. Los Angeles CA 90024

Little is known about the biochemical mechanism of K-channel phosphorylation in squid giant axons (PNAS 83:2743, 1986 and Biophys. J. 49:215a, 1986). In this preparation, the K conductance is dramatically modified in amplitude and kinetics by a phosphorylation reaction which requires ATP.

We have studied the effects of GTP and its non hydrolyzable form, GTP- $\gamma$ -S on the amplitude and kinetics of phosphorylated K-channels in dialyzed and voltage-clamped squid axons. In axons in which  $I_K$  is already maximally stimulated, the addition of 500  $\mu\text{M}$  of Mg-GTP further increases (5 to 8 %) the current and slows-down its kinetics. GTP- $\gamma$ -S causes the same effect but it is approximately 2- fold more effective than GTP. However, if  $I_K$  stimulation by ATP is not maximal, GTP- $\gamma$ -S potentiates even more (40 %). These results suggest that GTP is increasing the affinity of the phosphorylating system for ATP. When GDP is added to the fully stimulated  $I_K$  (2 mM ATP), the stimulation already present is greatly diminished, suggesting that GDP inhibits through the same pathway used by GTP and GTP- $\gamma$ -S. However, another inhibitory mechanism cannot be ruled out with the present results. The effect of GTP- $\gamma$ -S is irreversible whereas GTP action is not maintained even when GTP is present throughout the experiment.

The GTP effect is not the result of transformation of GTP into cGMP since the addition of cGMP to the dialysis fluid (in the presence of ATP) does not modify  $I_K$ . Neither GTP nor GTP- $\gamma$ -S affect  $I_K$  when the channels are dephosphorylated (0 ATP) and in the presence of GTP- $\gamma$ -S (or GTP) all modifications of  $I_K$  are of the same kind as ATP alone but more pronounced. These results show that GTP- $\gamma$ -S acts only as a potentiator of the ATP effect already present. In conclusion, GTP and GTP- $\gamma$ -S potentiate the phosphorylation of K-channels, probably through the activation of a GTP-binding protein that acts in the biochemical cascade responsible for this reaction. (Supported by USPHS GM 30376 and MDA).

**Th-AM-A9 MODULATION OF ATP-SENSITIVE K CHANNELS IN RINm5F CELLS BY PHOSPHORYLATION AND G PROTEINS.** B. Ribalet, S. Ciani and G.T. Eddlestone. Dept. of Physiology; BRI; JLNRC. Univ. of Calif., Los Angeles, CA 90024.

The regulation of ATP-sensitive K channel activity in insulin secreting RINm5F tumor cells was studied using patch-clamp techniques. A progressive run-down of channel activity, generally observed upon excision of inside-out patches, may be prevented by addition of low concentrations of ATP (10  $\mu\text{M}$ ) and GTP (100  $\mu\text{M}$ ) to the bath. That the stimulatory effect of low levels of ATP may be due to phosphorylation via protein kinase A is suggested by the following findings: 1) In the cell-attached patch, addition of dibutyryl-cAMP (50  $\mu\text{M}$ ) to the bath causes an increase of channel activity; 2) In the excised inside-out patch, addition of the catalytic subunit of protein kinase A (0.25  $\mu\text{M}$ ) stimulates the activity; 3) In the inside-out patch addition of a specific inhibitor of protein kinase A (5 to 15  $\mu\text{M}$ ) depresses channel activity. The effect of GTP appears to be mediated via guanosine nucleotide binding (G) proteins acting directly on the channel. In support of this proposal experiments using excised inside-out patches showed that: 1) addition to the bath of preactivated pertussis toxin (a toxin which inactivates the inhibitory G protein ( $G_i$ )) reduces channel activity in the presence of  $\text{NAD}^+$ ; 2) addition of 40 pM of a GTP- $\gamma$ -S activated  $\alpha$ -subunit of a  $G_i$  from human erythrocytes (kindly provided by L. Birnbaumer, J. Codina and A. Brown of Baylor College of Medicine) strongly enhances channel activity. Regulation by these two pathways seems to be required to maintain the channel in an active state, since we often observed that addition of ATP or GTP alone was not sufficient to prevent the run-down of channel activity. Whether these two pathways are independent or related is still unclear. Supported by a NSF grant DCB-85 17413, an award from the ADA (W-P860812) and a grant from the MDA.

**Th-AM-A10 MODULATION OF HEART DELAYED RECTIFICATION BY PROTEIN KINASE A AND C: EVIDENCE FOR DIFFERENT MECHANISMS OF ACTION.** K.B. Walsh and R.S. Kass, Department of Physiology, University of Rochester Medical Center, Rochester, NY 14642.

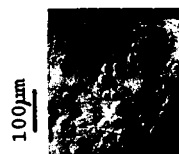
The cardiac delayed rectifier potassium current ( $I_K$ ) is regulated by protein kinase A and protein kinase C in a manner that depends steeply on cell temperature (*Science* 242: 67-69, 1988). In the present study, we have investigated the mechanisms by which stimulation of these two kinases modify the activity of this channel. We focused on  $I_K$  kinetics and the voltage-dependence of channel modulation during kinase stimulation.  $I_K$  was recorded from guinea pig ventricular myocytes using the whole cell arrangement of the patch clamp in an external solution containing (in mM): 140 N-methyl glucamine, 4.8 KCl, 1.2  $MgCl_2$ , 1  $CaCl_2$ , 5 dextrose, 10 HEPES, 5  $\mu M$  TTX and 200 nM nisoldipine (pH=7.4, temperature=35°C). Activation of  $I_K$  was measured during 2-3 s voltage pulses applied from a -30 mV holding potential, and  $I_K$  deactivation was monitored as tail current at the holding potential following the positive voltage pulses. Stimulation of protein kinase A by isoproterenol or the membrane permeable cAMP analog (8-chlorophenylthio cAMP) caused voltage-dependent enhancement of  $I_K$  amplitude and changes in  $I_K$  kinetics. The effects of kinase A stimulation on  $I_K$  amplitude were most pronounced at voltages negative to +20 mV (4-6 fold increase in  $I_K$ ) and became smaller at more positive voltages (2-fold increase at voltages between +20 and 100 mV). Concomitant with this action on  $I_K$  amplitude were changes in  $I_K$  kinetics. Deactivation was slowed at the holding potential and activation was slightly speeded at voltages between -10 mV and +30 mV. The kinetic changes induced by kinase A contribute to but cannot account entirely for the voltage-dependent actions on  $I_K$  amplitude. In contrast to these actions, stimulation of protein kinase C by phorbol 12,13 dibutyrate enhanced  $I_K$ , but in this case, the effects on  $I_K$  amplitude were more pronounced at voltages positive to +20 mV than at more negative potentials. In addition, protein kinase C stimulation did not affect the kinetics of  $I_K$  activation but sped deactivation of this channel at the holding potential. From our results we conclude that these two kinases regulate  $I_K$  by two different mechanisms which are consistent with distinct phosphorylation of two separate sites.

**Th-AM-A11 AXOBALLS: SPONTANEOUS FORMATION OF LARGE VESICLES AFTER INJURY OF SQUID AXONS.**

P.G. Stein, H.M. Fishman and K.P. Tewari, Department of Physiology and Biophysics, University of Texas Medical Branch, Galveston, TX 77550. (Introduced by B.H. Alderson)

Injury (by cutting, stretching or tearing) of giant axons in 3 species of squid and cuttlefish in ASW at 20°C initiates a complex set of events which include local contraction of the cytoskeleton, extrusion of axoplasm and our observation that numerous large vesicles form. The vesicles appear in the presence of divalent cations (10 mM/L Ca or Mg) and do not appear in their absence. High magnification phase contrast microscopy showed that vesicle formation occurs in a region very close to the axolemma making it appear likely that the source of the membrane is either the axolemma or sub-surface cisterns of the endoplasmic reticulum (ER). Vesicles are observed within minutes of axon transection in ASW and thereafter enter into fusions to produce larger vesicles with time (e.g. vesicles in Fig. are 20-30  $\mu m$  diameter after 15 minutes). In a transected axon, vesicles move toward the site of injury and accumulate at the constricted end where further fusions occur resulting in the emergence of giant membranous balls (maximum size 250  $\mu m$  diameter). These results suggest that vesiculation plays a role in the immediate cellular response to axonal injury. As discussed in the accompanying abstract these balls can be studied by the patch clamp technique. (see also poster presentation) Aided by ONR contract N000-14-87-K-0055.

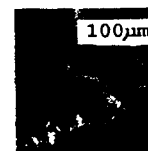
We thank Dr. Roger T. Hanlon for supplying cephalopods through NIH grant RR01024.



**Th-AM-A12 AXOBALLS: A MODEL ION CHANNEL PREPARATION FROM THE SQUID GIANT AXON.**

H.M. Fishman, P.G. Stein and K.P. Tewari, Department of Physiology and Biophysics, University of Texas Medical Branch, Galveston, Texas 77550.

As described in the accompanying abstract, giant membranous balls emerge from an axon after injury. Patches of membrane on the surface of these balls can be electrically isolated (30-100 gigaohms) from the surrounding medium with electrolyte-filled glass pipets (see Fig.) allowing low noise recording of patch currents. In excised inside-out patches we observed a variety of stochastic current waveforms for steady-state voltage clamps between  $\pm 100$  mV. With ASW in the bath and 440 K-ASW in the pipet (and TTX, 1  $\mu M/L$ , on both sides), fluctuations between two levels, reflecting conduction in single channels, were recorded at 24°C. The current-voltage relation was linear over the range 50 to 85 mV (pipet-bath) and gave a conductance of 12 pS and an extrapolated reversal potential of -50 mV. Addition of 1 mM/L Zn to the bath severely limited channel openings. Because this amount of Zn added to the bath of intact axons reversibly reduced K current by 65% and because fluctuations similar to those in ASW were recorded when Cl was replaced on both sides by glutamate, this channel appears to be a K channel. Other recordings show channels with multiple conducting states and stochastic fluctuations reflecting conduction of many channels. All channel activity ceased 30 min after addition of 0.1% glutaraldehyde to the bath. These channels appear to come from either the axolemma or ER. Whichever is the source, axoballs provide a model ion channel preparation derived directly from the squid axon without biochemical intervention. Aided by ONR contract N000-14-87-K-0055.





**Th-AM-B1** CALCIUM BINDING AND CONFORMATION CHANGE OF TROPONIN-C EXPLORED BY SITE-DIRECTED MUTAGENESIS. T. Borgford, K. Golosinska, L.B. Smillie, C.M. Kay and B.D. Sykes; MRC Group in Protein Structure and Function, Department of Biochemistry, University of Alberta, Edmonton, Alberta, Canada T6G 2H7.

Site-specific mutants of chick skeletal muscle troponin-C were prepared and expressed in *E. coli* as described (Reinach, F.C. and Karlsson, R. (1988) *J. Biol. Chem.* 263, 2371-2376). Chicken troponin-C does not naturally contain either Trp or Tyr residues. Consequently, it was possible to assign, unambiguously, spectroscopic properties to Trp or Tyr which had been introduced into the protein by mutagenesis. Tyr was substituted for Met-48, between binding sites I and II, and became a "reporter" of conformational change. The proposed model (Herzberg, O., Moulton, J. and James, M.N.G. (1986) *J. Biol. Chem.* 261, 2638-2642) for the transition from the apo to the  $\text{Ca}^{2+}$  bound form suggested that Met-48 would become more exposed to solvent in the binding of  $\text{Ca}^{2+}$  to the low-affinity sites. However, spectral (CD, difference UV) and NMR analyses indicated that the environment of the Tyr becomes more "chiral" and nonpolar and less mobile as  $\text{Ca}^{2+}$  binds. A further mutant was prepared in which Phe 29 was replaced by Trp. The fluorescent yield was increased 300% upon  $\text{Ca}^{2+}$  binding. The half saturation point of the fluorescence at a  $\text{pCa}^{2+}$  of 5.1 was close to that expected previously from reported values of the binding constants for the low affinity sites. The data were not, however, consistent with the titration of identical independent sites but exhibited a high degree of cooperativity with a Hill coefficient of approximately 2. The pronounced concave curvature of Scatchard plots also indicated strong positive cooperativity and was evident over a wide range of protein concentration. (Supported by the Alberta Heritage Foundation for Medical Research and the Medical Research Council of Canada.)

**Th-AM-B2** BARNACLE TROPONIN C: AMINO ACID SEQUENCES OF THE TWO ISOFORMS. J.H. Collins\*, J.L. Theibert\*, J.D. Potter# and C.C. Ashley#. \*Dept. Biological Chemistry, Univ. Maryland School of Medicine, Baltimore, MD 21201, #Dept. Pharmacology, Univ. Miami School of Medicine, Miami, FL 33101, and §Univ. Lab. Physiology, Oxford OX1 3PT, UK.

We previously reported (Potter et al., *Biophys. J.* 51: 329a, 1987) the purification and preliminary characterization of major (BTnC-2) and minor (BTnC-1) isoforms of troponin C from the giant barnacle *Balanus nubilis*. We have now completed sequence analyses of BTnC-1 and BTnC-2, using protein chemistry methods. BTnC-2 contains 151 amino acid residues, while BTnC-1, due to an elongated N-terminus, contains 158. The two sequences can be easily aligned, using no insertions or deletions, with vertebrate skeletal TnC sequences. The barnacle sequences, however, are only 60% identical to one another. Differences are much more frequent in the N-terminal than in the C-terminal halves, but occur in all regions of the polypeptides. This indicates that BTnC-1 and BTnC-2 are products of different genes, rather than alternative transcripts of a single gene. Internal sequence repeats show that both isoforms contain the usual four ancestral Ca-binding domains, numbered I to IV from the N-terminus. BTnC-1 and BTnC-2 both appear from their sequences to have functional Ca-binding sites in domains II and IV. In addition, BTnC-1 may bind Ca weakly in domains I and III. Only BTnC-2 can be labeled with dansylaziridine, probably because it contains a cluster of Met residues (not present in BTnC-1) in the N-terminal segment that preceded domain I. BTnC-2, but not BTnC-1, contains a single Cys residue, located in domain I, which is not labeled. (Supported by grants from the MDA, NSF and NIH.)

**Th-AM-B3** INTRAMOLECULAR CROSSLINKING IN TROPONIN C. Z. Grabarek, Y. Mabuchi and J. Gergely. Dept. of Muscle Res. Boston Biomed. Res. Inst.; Depts. of Neurology, and Biol. Chem., Harvard Medical School and Dept. of Neurology Mass. General Hosp. Boston MA.

Recent data obtained on model synthetic peptides indicate that electrostatic interactions between amino acid side chains carrying opposite charges and located on adjacent turns of an  $\alpha$ -helix (positions  $i$  and  $i+4$  of the sequence) strongly stabilize the  $\alpha$ -helical structure (Marqusee, S and Baldwin, R. *Proc. Natl. Acad. Sci. USA* 84, 8898, 1987). With respect to the three dimensional structure of troponin C (TnC) Sundaralingam et al. (*Proc. Natl. Acad. Sci. USA* 82, 7944, 1985) have suggested that several such interactions may stabilize its most unusual feature - the single stranded central  $\alpha$ -helix. To further explore this hypothesis and in search of the physiological importance of the central helix we have studied properties of TnC intramolecularly crosslinked with a zero length crosslinker 1-ethyl-3-[3-dimethylamino] propyl-carbodiimide (EDC). Upon treatment with EDC TnC undergoes multiple intramolecular crosslinking as indicated by a characteristic pattern of bands on electrophoresis under denaturing conditions (presence of SDS or 6M urea and EDTA). The pattern of the crosslinked bands is different depending on whether the crosslinking is performed in the presence of  $\text{Ca}^{2+}$  or  $\text{Mg}^{2+}$  suggesting that specific conformers are being trapped. Most of the crosslinked species are able to bind TnI and TnT and some bind stronger than unmodified TnC. Upon crosslinking the  $\alpha$ -helix content of TnC is increased in the absence of  $\text{Ca}^{2+}$  while in the presence of  $\text{Ca}^{2+}$  remains essentially unchanged. We are currently attempting to determine the positions of crosslinks in selected crosslinking products. Supported by grant from NIH (HL-05949) and American Heart Association.

**Th-AM-B4 PROBING THE MECHANISM OF THIN FILAMENT REGULATION BY TROPONIN USING A PEPTIDE PATCH.**

Z. Grabarek, J. Gergely and P.C. Leavis, Dept. Muscle Research, Boston Biomedical Res. Inst., Mass. General Hospital and Harvard Medical School. Boston MA 02114.

Calcium addition to troponin induces changes in the complex characterized by a "tightening" of the interaction between the TnC and TnI subunits. Evidence surfacing in recent years suggest that this tightening involves a  $\text{Ca}^{2+}$ -dependent interaction between a region of TnC comprising residues 89-100 and TnI residues 96-116, and that this interaction is an essential event in the regulatory process (Grabarek et al. J. Biol. Chem. 261,608,1986). To shed further light on the significance of the interaction we have covalently crosslinked the TnI peptide corresponding to residues 96-116 (peptide CN4) to TnC using a two step process involving activation of the carboxylate side chains of TnC followed by addition of the peptide to form zero-length crosslinks (Grabarek and Gergely Biophys. J. 53,392,1988). The crosslinked product is a 1:1 TnC-CN4 complex as indicated by PAGE in the presence of SDS and by electrophoresis on an alkaline urea gel. The "patched" TnC is still able to bind intact TnI and to form a ternary troponin complex which suggests that other sites of interaction between the troponin subunits are not affected by the crosslinking. Reconstituted thin filaments containing TnC-CN4 are unable to activate myosin S1 ATPase upon addition of  $\text{Ca}^{2+}$  providing further evidence for the importance of the interaction between residues 89-100 of TnC and TnI in regulation. These data suggest that a peptide patch crosslinked to its target site can impair a specific function attributed to a protein-protein interaction and thus can provide information about its functional significance. Supported by grants from NIH (HL-05949, HL-20464) and by Muscular Dystrophy Association.

**Th-AM-B5 MEASUREMENT OF  $\text{Ca}^{2+}$  BINDING TO DIFFERENT CALCIUM BINDING PROTEINS USING NEW FLUORESCENT  $\text{Ca}^{2+}$  INDICATORS.** Jean-Marie Francois and James D. Potter, Dept. of

Pharmacology, Univ. of Miami School of Medicine, P.O. Box 016189 Miami, FL 33101.

Recently, several groups have produced TnC by recombinant DNA technology which allows site-directed mutagenesis of it. Although a few mutant TnC's have been synthesized so far, one can expect the production of an increasing number of them. These mutant TnC's will allow the investigation of structure-function relationships in this protein. The first step before studying biological activity of these mutant TnC's is to investigate their physical-chemical properties and particularly their affinity for  $\text{Ca}^{2+}$ . Thus, we are currently developing a simple method to measure the  $\text{Ca}^{2+}$  affinity of TnC (and other  $\text{Ca}^{2+}$  binding proteins). The use of fluorescent  $\text{Ca}^{2+}$  indicators is particularly useful to measure the free  $\text{Ca}^{2+}$ . Due to a high quantum yield of these fluorophores, a concentration of 1  $\mu\text{M}$  of the  $\text{Ca}^{2+}$  indicator is enough to give a strong fluorescence signal. In this way, the low concentration of protein (20-60  $\mu\text{M}$  for TnC) needed is another advantage to this method. Compared to equilibrium dialysis, our method is faster (typically 1h) and consumes only small quantities of protein. Recently, new  $\text{Ca}^{2+}$  indicators, Rhod-2 and Fluo-3, have been developed (Tsien and Minta (1987) J. Cell. Biol. 105,89a). They have a high  $K_d$  (1000 and 450 nM respectively) and can be used to measure the binding of  $\text{Ca}^{2+}$  to rabbit skeletal muscle TnC the results of which are shown in the Table. As can be seen, when Rhod-2 is used, the results we obtained are comparable to those utilizing equilibrium dialysis. We will also present data using other  $\text{Ca}^{2+}$  binding proteins and  $\text{Ca}^{2+}$  indicators.

	$\text{Ca}^{2+}$ indicator	equilibrium dialysis*	
Rhod-2	$n_1 = 2.1$ sites, $K_1 = 6.5 \cdot 10^7 \text{ M}^{-1}$ $n_2 = 2.2$ sites, $K_2 = 3.9 \cdot 10^5 \text{ M}^{-1}$	$n_1 = 1.8$ sites, $K_1 = 2.1 \cdot 10^7 \text{ M}^{-1}$ $n_2 = 2.1$ sites, $K_2 = 3.2 \cdot 10^5 \text{ M}^{-1}$	Supported by grants from NIH and MDA. *(Potter and Gergely (1975) J. Biol. Chem. 250, 4628).

**Th-AM-B6 EFFECT OF THROMBIN FRAGMENTS OF RABBIT TnC ON TnC DEPLETED SKINNED MUSCLE FIBERS FROM RABBIT.** Zelin Sheng, Jean Marie Francois and James D. Potter, Dept. of Pharmacology, Univ. of Miami School of Medicine, P.O. Box 016189 Miami, FL 33101.

Proteolytic fragments of TnC have been useful in analyzing the relationship between the structure and function of TnC. Three thrombin fragments, TH<sub>I</sub> (residue 1-120), TH<sub>II</sub> (121-159) and TH<sub>III</sub> (101-120) were prepared. TnC depleted skinned fibers were incubated with each fragment (20  $\mu\text{M}$ ) at pCa 4 or 8, then incubated with rabbit TnC (4  $\mu\text{M}$ ), re-extracted with EDTA and incubated with rabbit TnC. Each step was followed by washing at pCa 8.0 and recording force at pCa 4.0. Parallel experiments were done with rabbit TnC (RTnC), Parvalbumin (Parv), and calmodulin (CaM) and are shown in the Table. CaM restored tension at pCa 4 but did not block TnC rebinding and Parv did neither. TH<sub>I</sub> (Ca binding sites I, II, III) added at pCa 4 activated but did not block TnC rebinding, and at pCa 8 little effect was seen. TH<sub>II</sub> (Ca binding site IV) had little effect at either pCa. TH<sub>III</sub> (Ca binding site III) had a slight activating effect at pCa 4, but after pCa 8 washing inhibited rebinding of TnC. We conclude that the entire structure of TnC is needed for full function, although partial activities can be seen with some of the fragments. Supported by grants from the NIH and MDA.

	RTnC pCa 8	Parv pCa 8	pCa 4	CaM pCa 8	pCa 4	TH <sub>I</sub> pCa 8	pCa 4	TH <sub>II</sub> pCa 8	pCa 4	TH <sub>III</sub> pCa 8	pCa 4
restore tension	+++	-	-	-	+++	+/-	++	-	+/-	-	+
block TnC rebinding	-	-	-	-	-	-	+/-	-	+/-	-	++
	- = 0%	+/- = 0-10%		+ = 10-30%		++ = 30-60%		+++ = more than 60%			

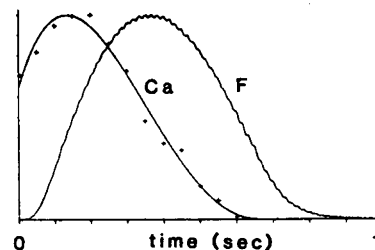
**Th-AM-B7 CHANGES IN TROPONIN T ISOFORMS MODULATE  $\text{Ca}^{2+}$  BINDING AND ACTIVATION OF FORCE GENERATION IN THE DEVELOPING MYOCARDIUM.**

J. J. McAuliffe\* and R.J. Solaro#. Dept. of Anesthesia\*, University of Cincinnati College of Medicine, Cincinnati, Ohio; Dept. of Physiology and Biophysics#, University of Illinois at Chicago, Chicago, Illinois.

We had previously reported that the binding of  $\text{Ca}^{2+}$  to cardiac myofibrils changed with postnatal age. Those data were fit to two types of models for  $\text{Ca}^{2+}$  binding to TnC called H2L1 and HL1L, where H is the number of high affinity sites and L the number of low affinity sites. The HL1L model requires that one of the high affinity sites be closed after binding occurs to the other. Skinned fibers were prepared from hearts of the same age and pCa force curves derived fixing initial sarcomere length with a Ne-He laser when possible. PAGE analysis and immunoblots were used to determine myofibrillar protein composition. Quantitative TnC measurements were identical in both groups and averaged 0.45 nmole/mg protein. The 22d  $\text{Ca}^{2+}$  binding data fit a classic model for 3  $\text{Ca}^{2+}$  binding sites per mole TnC ( $K_1=1.4 \times 10^7 \text{M}^{-1}$ ;  $K_2=3.3 \times 10^5$ ); the 5d data gave the best fit to the HL1L model (2  $\text{Ca}^{2+}$  binding sites/mole TnC), yielding  $\text{Ca}^{2+}$  binding constants of  $K=1.7 \times 10^7 \text{M}^{-1}$ ;  $K_2=1.03 \times 10^6$ . The HL1L model allows the low affinity site of TnC in the 5d myofibrils to maintain its regulatory role, whereas the H2L1 would not. The pCa-force data indicated that the pCa50 was not different but the Hill coefficient was greater (3.1 vs 2.1) for the 5d group. The only significant difference on PAGE analysis was the presence of a TnT doublet in the 5d group not in the 22d group. The pattern of  $\text{Ca}^{2+}$  binding and activation appears to be a function of the TnT isotype present.

**Th-AM-B8 ESTIMATED TIME COURSE OF CALCIUM BOUND TO TROPONIN DURING ISOMETRIC RELAXATION IN RABBIT PAPILLARY MUSCLE.** JN Peterson, WC Hunter & MR Berman. The Johns Hopkins University, Baltimore, Md. 21205.

Muscle relaxation involves the interaction of two processes: 1) removal of calcium ( $\text{Ca}^{2+}$ ) bound to troponin C (TnC), and 2) crossbridge detachment. An estimate of bound  $\text{Ca}^{2+}$  would allow one to separate these processes, but no methods are currently available for monitoring bound  $\text{Ca}^{2+}$  in intact cardiac muscle. Therefore, we devised an assay using mechanical perturbations. An impulse (stretch, then release) in muscle length of magnitude  $4.2 \pm 1.0\% L_{\text{max}}$  was used to detach all crossbridges at different times during an isometric twitch. We reasoned that if any force redeveloped after the impulse, then some calcium must still be bound to TnC. A simple model suggested that the time course of the initial derivative of redeveloped force after the impulse, as a function of impulse time, was representative of the time course of bound  $\text{Ca}^{2+}$ . Using this derivative measure, we found that bound  $\text{Ca}^{2+}$  was insignificant (less than 10% of maximum) after force had declined only slightly to  $78 \pm 12\%$  (mean  $\pm$  s.d.,  $n=13$ ) of peak. It is concluded that, in rabbit papillary muscle at  $24^\circ\text{C}$ , a substantial portion of relaxation is independent of bound  $\text{Ca}^{2+}$ . Supported by HL38488 (MRB).



**Th-AM-B9 COOPERATIVE  $\text{Ca}^{2+}$  BINDING TO RECONSTITUTED AND NATIVE CARDIAC THIN FILAMENTS.**

LS Tobacman and D Sawyer, University of Iowa College of Medicine, Iowa City, IA 52242.

$\text{Ca}^{2+}$  binds cooperatively to reconstituted cardiac thin filaments containing IAANS-modified troponin C. A theoretical model suggests that both the cooperativity of binding and the average  $\text{Ca}^{2+}$  affinity per regulatory site depend upon interactions between neighboring troponin-tropomyosin-7 actin units. Because of these interactions,  $\text{Ca}^{2+}$  is four times ( $Y=4$ ) more likely to elongate an activated stretch of the thin filament than to bind in the middle of an inactivated segment. The midpoint of the binding curve is determined by two factors: (1) the  $\text{Ca}^{2+}$  affinity of a theoretically isolated site; (2) the different interaction free energies between either two units both binding  $\text{Ca}^{2+}$  or two units not binding  $\text{Ca}^{2+}$ . Thin filament  $\text{Ca}^{2+}$  binding (fluorescence change) closely corresponds to MgATPase rate activation of low concentrations of myosin S-1. Therefore, MgATPase rate vs. pCa data are indirect measures of regulatory site  $\text{Ca}^{2+}$  binding. Native thin filaments (Ngai, et al, Biophys J 53:585a) and reconstituted thin filaments produce similar  $\text{Ca}^{2+}$ -induced myosin S-1 MgATPase rate cooperativity ( $Y=4$ ,  $n_H=2$  vs.  $Y=3.7$ ,  $n_H=1.8$ ). Using MgATPase rate data, reconstituted thin filaments have a 5-fold stronger apparent  $\text{Ca}^{2+}$  affinity than native thin filaments. This difference is not altered by dephosphorylation of troponin I. However, incubating native thin filaments with a 10-fold molar excess of purified troponin raises the  $\text{Ca}^{2+}$  affinity to that of reconstituted thin filaments. These results suggest that cooperative  $\text{Ca}^{2+}$  binding to reconstituted cardiac thin filaments reflects the cooperativity of native thin filaments, but that the reconstituted system has an altered  $\text{Ca}^{2+}$  affinity due to an unexplained difference in troponin.

**Th-AM-B10** EFFECTS OF ACIDIC pH ON CA-BINDING TO THE REGULATORY SITE OF CARDIAC TROPONIN C. Saleh C. El-Saleh and R. John Solaro, Depts. of Physiology and Biophysics, University of Cincinnati, Cincinnati, OH 45267 and University of Illinois, Chicago, IL 60680.

Ca-activated ATPase activity, force, and Ca-binding are inhibited when the pH surrounding cardiac myofibrils is reduced. To more completely understand the mechanism(s) of this inhibition, we have tested whether Ca-binding to the regulatory site on cardiac troponin C (CTNC) is directly influenced by elevations in proton concentration, as is the case in fast skeletal TNC (El-Saleh and Solaro, J. Biol. Chem. 263:3274-3278, 1988). Measurements were made using preparations of CTNC, labelled with the fluorescent probe IAANS, which reports Ca-binding to the regulatory site. Our results show that protons can not only directly depress Ca-binding to CTNC, but also that for the same 0.5 unit drop in pH, the Ca-binding to the CTNC regulatory site is depressed 4 fold as compared to 1.6 fold in skeletal TNC. Moreover, we found that this effect of acidic pH on CTNC is dramatically depressed in its complex with cardiac troponin I (CTNI). Addition of CTNI to CTNC reduced the effect of acidic pH 17 fold in the case of cardiac preparations, but only about 4 fold in the case of skeletal preparations. In fact, the acidic pH induced desensitization of skeletal myofibrillar ATPase activity was essentially abolished when native skeletal TNC was replaced with CTNC. Our results indicate that the degree of inhibition of myofilament activity by acidic pH is a property of the variant of TNC present and its interactions with its neighbors in the thin filament, especially TNI. Supported by NIH grant HL 22231 (RJS) and by a grant from the AHA-Ohio affiliate (SCE).

**Th-AM-B11** IDENTIFICATION OF TROPONIN-I ISOFORMS IN DEVELOPING RAT HEARTS. Pankaj Kumar, Ann F. Martin and R. John Solaro (Spon. by Mrinalina Rao) Depts. of Physiology and Biophysics, and Department of Pharmacology and Cell Biophysics, University of Cincinnati, Cincinnati, OH 45267 and Dept. of Physiology and Biophysics, University of Illinois, College of Medicine at Chicago, Chicago, IL 60680.

Comparison of the protein profiles of myofibrils isolated from adult rat hearts and rats in the neonatal period before weanling show evidence for isoforms of troponin I (TNI), the inhibitory component of the TN complex. We have observed two putative "developmental" forms of rat cardiac TNI, that migrate with slower mobility on SDS-PAGE than the "adult" form. We have identified these components of the neonatal myofibrils as TNI by cross-reactivity with a polyclonal antibody to skeletal TNI and by binding to cardiac troponin C. The relative abundance of the developmental isoforms is correlated with a relative insensitivity of myofibrillar Ca-activation to inhibition by acidic pH (Solaro et. al. Circ. Res., In Press). Moreover, Ca-activation of hybrid regulated actomyosin prepared by substitution of the troponin-troponin complex of the neonatal heart myofibrils with purified troponin-tropomyosin shows sensitivity to acidic pH similar to that of the adult preparations. Our results indicate that during development in the neonatal period that rat heart myofibrils possess a population of isoforms of TNI, and that the distribution of isoforms in this population may be related to the relative insensitivity of the neonatal myofilaments to deactivation by acidic pH. Supported by NIH HL 22231 and HL 22619 IIB.

**Th-AM-B12** EVIDENCE FOR A ROLE OF TROPONIN T IN THE CALCIUM REGULATION OF TENSION PRODUCTION IN MAMMALIAN SKELETAL MUSCLE. Peter J. Reiser, Marion L. Greaser\* and Richard L. Moss, Department of Physiology and \*Muscle Biology Laboratory, University of Wisconsin, Madison, WI 53706.

We examined the troponin (Tn) and tropomyosin (Tm) subunits of 4 day neonatal and adult rabbit soleus (S) and psoas (P) muscles and the tension/pCa relations of single fibers from these muscles. The objective was to determine if developmental transitions in Tn and Tm of mammalian muscle are related to changes in the  $\text{Ca}^{2+}$ -sensitivity of tension production. Tn and Tm subunits were studied using SDS-PAGE. Neonatal and adult S and P muscles contained both  $\alpha$  and  $\beta$  Tm with the  $\alpha:\beta$  ratio  $\gg 1$  in adult P,  $< 1$  in adult S and  $\sim 1$  in neonatal S and P. Adult S and P muscles contained isoforms of TnT, TnC, and TnI that were either slow-type or fast-type, respectively. Neonatal P contained almost exclusively the fast-type isoforms of TnC and TnI while more equal mixtures of slow-type and fast-type were found in neonatal S. Neonatal S and P did not contain any detectable fast-type TnT. Both S and P neonatal muscles contained two other isoforms of TnT, one of which co-migrated with the single, adult slow-type isoform and the other form represented at least half of the TnT in both neonatal muscles. Greater amounts of  $\beta$ Tm were associated with slow-type TnT. Preliminary tension/pCa data indicate that neonatal S and P and adult S all have similar  $\text{Ca}^{2+}$ -sensitivities; adult P has a higher threshold for activation and an apparent higher degree of cooperativity (i.e., steeper tension/pCa relation). We conclude that TnT isoforms, possibly along with Tm, have a major role in determining the  $\text{Ca}^{2+}$ -sensitivity of tension production in mammalian muscle since a combination of predominantly fast-type TnC and TnI with slow-type TnT is associated with a tension/pCa relation characteristic of adult slow muscle. Supported by NIH.

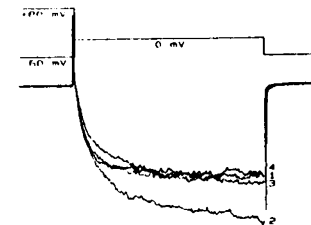
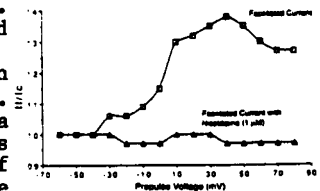
**Th-AM-C1 HIGH AFFINITY AND TISSUE SPECIFIC BLOCK OF T-TYPE Ca CHANNELS BY FELODIPINE.**

D.M. Van Skiver, Sherrill Spires and C.J. Cohen, Merck Institute, Rahway, NJ 07065

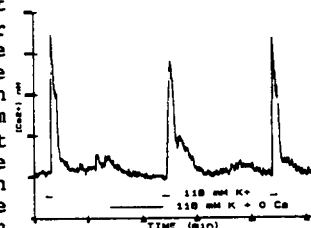
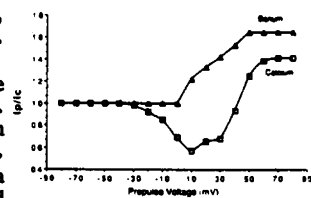
The two types of Ca channel current in guinea pig atrial cells can be separated and quantitated by analyzing the current measured when the membrane is repolarized after a brief depolarization (tail current analysis). As in some other types of excitable cells, the T-type Ca channels in atrial cells deactivate slowly when the membrane is repolarized and the L-type Ca channels deactivate rapidly. Tail current analysis was used to concurrently study block of both types of Ca channels over a broad range of voltages. The 1,4-dihydropyridine felodipine potently blocks T-type Ca channels in guinea pig atrial cells. Block is voltage dependent; the effective dissociation constant decreases as the fraction of channels that are inactivated increases. The voltage and concentration dependence of block are accounted for by a form of the modulated receptor theory that postulates preferential binding of felodipine to inactivated T-type Ca channels. The dissociation constant for inactivated channels ( $K_I$ ) is 14 nM. High affinity block by felodipine of T-type Ca channels is tissue specific; in GH<sub>3</sub> cells,  $K_I = 0.7 \mu\text{M}$ . Felodipine can block L-type Ca channels in atrial cells more potently than T-type Ca channels, but block of L-type Ca channels is potent only when binding equilibrates at depolarized potentials. For part of the physiologically relevant voltage range ( $V < -50 \text{ mV}$ ), felodipine either increases current through the L-type Ca channels or blocks the L-type Ca channels with potency similar to that for block of T-type Ca channels. Felodipine is the most potent blocker of T-type Ca channels reported to date and studies with this drug indicate that some of the pharmacological effects of 1,4-dihydropyridines may derive from block of T-type Ca channels.

**Th-AM-C2 FACILITATION OF CALCIUM CURRENT IN BOVINE CHROMAFFIN CELLS: RECRUITMENT OF A DIFFERENT CLASS OF CALCIUM CHANNELS? C.R. Artalejo, M. Dahmer, R.L. Perlman, A.P. Fox (Intr. by G. Jamieson), Dept. of Pharmacol. and Physiol. Sci., Univ. of Chicago, 947 E. 58th St., Chicago, IL 60637**

Facilitation of calcium currents by a prior depolarization pulse has been previously described in chromaffin cells (Fenwick et al., J. Physiol. 331, 1982; Hoshi et al., Proc. Natl. Acad. Sci. 81, 1984) and may represent a unique type of synaptic plasticity. The present data further characterize this phenomenon and suggest that this represents the recruitment of a new class of Ca channels rather than a novel property of a single type of Ca channel. The Ca currents in chromaffin cells were studied using a 2 pulse protocol in whole-cell patch clamp. This effect became progressively greater with more positive prepulse (P1) voltages (upper fig.). The facilitated current (lower fig.; #2) was completely blocked by superfusion of the cell with  $1 \mu\text{M}$  nisoldipine (#3), yet nisoldipine had no effect on the non-facilitated control current (#1,4). Three specific properties differentiate between the two currents and suggest that facilitation may be due to the recruitment of a second class of Ca channels; a) the deactivation pattern, b) inactivation properties, and c) sensitivity to dihydropyridines. Artalejo et al., (Biochem. Biophys. Res. Comm. 134, 1986) have previously shown that Ca influx through calcium channels precedes noradrenaline release, indicating that channel activity tightly modulates the kinetics of the secretory response. It would be interesting to know which of these Ca currents modulates the secretory response.

**Th-AM-C3 CALCIUM BUT NOT VOLTAGE-DEPENDENT INACTIVATION OF CALCIUM CURRENT AND INFLUX IN BOVINE CHROMAFFIN CELLS. L.D. Hirning, C.R. Artalejo, M. Dahmer, R.L. Perlman and A.P. Fox, (Intr. by J. Makielski) Dept. of Pharmacol. and Physiol. Sci., Univ. of Chicago, 947 E. 58th St. Chicago, IL 60637**

Calcium current inactivation has been characterized as either voltage dependent or a combination of voltage- and calcium-dependent processes. However, the present data indicate that only calcium-dependent inactivation is present in chromaffin cells. Previous studies (Artalejo et al., J. Biol. Chem. 262, 1987) have demonstrated that neither voltage changes nor Ca flux via Ca channels is responsible for channel inactivation. Rather, localized increases in intracellular Ca appear to determine the rate of inactivation of these channels. Maintained voltage clamp depolarization using Ca as the charge carrier produced dramatic and rapid inactivation of whole cell currents, yet with Ba as the charge carrier, little or no inactivation was observed (upper fig). Using the Ca indicator Fura-2, we have substantiated the lack of voltage dependent inactivation in these cells.  $K^+$  depolarization induced a rapid rise in intracellular Ca similar to that seen in peripheral neurons. However, with long depolarizations (10 min.) in the absence of external Ca, the calcium transient produced by the restoration of Ca was not significantly different from the preceding control (lower fig). The effects on catecholamine release are nearly identical.  $K^+$  depolarization in the absence of Ca does not diminish the release which occurs upon restoration of external Ca. The results of the data using all the three techniques strongly suggest that Ca channels in chromaffin cells show no voltage dependent inactivation.



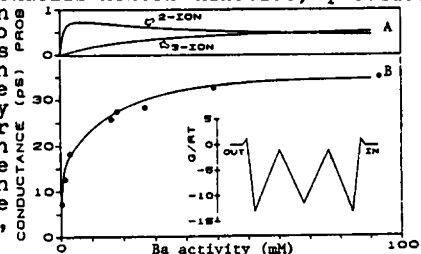
**Th-AM-C4 TRIFLUOPERAZINE ENHANCES  $\text{Ca}^{2+}$  DEPENDENT INACTIVATION OF  $\text{Ca}^{2+}$  CURRENTS IN HELIX NEURONS.**

Alvarez-Leefmans, F.J., Cruzblanca, H. and Bernal, J. Department of Pharmacology. CINVESTAV del IPN. Ap. Postal 14-740, México 07000, D.F. and Instituto Mexicano de Psiquiatría, Department of Neurobiology, Calz. México-Xochimilco 101, México 14370, D.F.

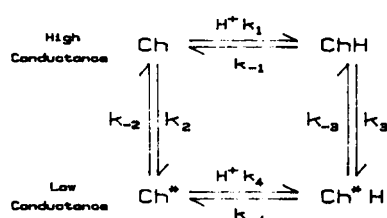
In previous studies (Biophys. J. 51, 33a, 1987) we found that trifluoperazine (TFP) reversibly reduces the amplitude of  $\text{Ca}^{2+}$  inward current ( $\text{ICa}^{2+}$ ) generated in *Helix* neurons by voltage clamp pulses from a holding potential ( $\text{Hp}$ ) of -50 mV. This effect was dose-dependent (5-50  $\mu\text{M}$ ) and was not due to changes in surface potential. Here we report that TFP (50  $\mu\text{M}$ ) enhances  $\text{Ca}^{2+}$  dependent inactivation of  $\text{ICa}^{2+}$  as shown in two pulse experiments in which P1 was varied in 10 mV steps from an  $\text{Hp}$  of -50 mV, P2 was fixed at the value of  $\text{I}_{\text{max}}$ , and the interval between P1 and P2 was fixed at 200 ms. Experiments were done in neurons (1D, 77F) from suboesophageal ganglia of *Helix aspersa* under two micro-electrode voltage clamp, after suppression of outward currents by Cs-loading, TEA and 4AP. The effectiveness of  $\text{Ca}^{2+}$  dependent inactivation was assessed from plots of normalized I2 vs Q1, where I2 is the peak  $\text{ICa}^{2+}$  generated by P2, and Q1 is the total amount of charge entering during P1. Normalized I2 vs Q1 plots revealed that 15 to 60 min. after exposure to TFP, the same amount of  $\text{Ca}^{2+}$  entering during P1 had an enhanced inactivatory effect on I2, as compared to controls. Enhancement of inactivation persisted even after recovery of  $\text{ICa}^{2+}$  amplitude during TFP washout. Activators of protein kinase C had no effect on  $\text{Ca}^{2+}$  dependent inactivation but produced an increase in  $\text{ICa}^{2+}$  (unpublished experiments done with C. Regen). It is suggested that TFP affects some  $\text{Ca}^{2+}$ /calmodulin process involved in the regulation of  $\text{Ca}^{2+}$  dependent inactivation of  $\text{Ca}^{2+}$  channels. Sponsored by CONACyT PCEXCA-030834 grant to F.J.A.L.

**Th-AM-C5 ION PERMEATION IN L-TYPE  $\text{Ca}$  CHANNELS: EVIDENCE FOR TRIPLE-ION OCCUPANCY IN THE CONDUCTION PATHWAY.** Eduardo Marban and David T. Yue<sup>1</sup>. Depts. of Medicine (Cardiology) and Biomedical Engineering<sup>1</sup>, The Johns Hopkins University School of Medicine, Baltimore, MD 21205

One of the simplest models that explains the remarkable conduction properties of L-type  $\text{Ca}$  channels envisions the permeation pathway as a multi-ion, single-file pore. However, we find no evidence for one of the crucial experimental buttresses of this theory: the anomalous mole fraction effect between Ba and Ca. In single-channel recordings from guinea-pig ventricular myocytes, neither conductance nor absolute unitary current (at 0 to -100 mV) exhibits a paradoxical decrease when Ba and Ca are mixed, with the total concentration of Ba + Ca kept constant at 10 (or 110) mM. To obtain independent evidence to support or reject the multi-ion theory, single-channel conductance was determined in cell-attached patches as Ba concentration in the pipette was varied between 1 and 400 mM. When viewed over such a large range, the conductance-activity relation (B, means pooled from 20 patches) demonstrates an initial rapid rise, followed by a failure to reach saturation in high Ba ("creep"). This pattern, clearly inconsistent with Michaelis-Menten kinetics, provides independent support favoring multi- over single-ion permeation models. Interestingly, 2-binding-site models inevitably fail to predict the creep phase. This characteristic discrepancy suggests that there are  $> 3$  binding sites in the permeation pathway. In fact, a 3-site model (B, inset) nicely predicts the conductance data (B, solid curve). As shown in A, rapid 2-ion occupancy produces the brisk rise in conductance at low Ba, while a slower rise in 3-ion occupancy leads to the secondary creep. Single-ion occupancy is not correlated with a measurable rising phase because channels populated with one divalent cation are blocked with respect to monovalent fluxes. Thus, we propose that cardiac L-type  $\text{Ca}$  channels can bind 3 or more ions simultaneously in the pore, despite the absence of anomalous effects between Ba and Ca.

**Th-AM-C6 A MODEL FOR THE PROTON-INDUCED CONDUCTANCE FLUCTUATIONS IN L-TYPE CALCIUM CHANNELS.** Daniela Pietrobon, Blaise Prod'homme & Peter Hess, Dept. of Cell. & Mol. Physiology, Harvard Medical School, Boston, MA 02115.

Analysis of the lifetimes of the two conductance levels, which are observed in open L-type  $\text{Ca}$  channels when monovalent ions carry the current, shows that the mean dwell time at the high conductance decreases linearly with increasing proton activity ( $a_{\text{H}^+}$ ) whereas the mean time spent at the low conductance increases with  $a_{\text{H}^+}$ . This result cannot be explained by a two state model, in which the two conductance states represent the protonated and unprotonated channel, and argues against mechanisms in which the presence of the proton at its site causes the reduced conductance directly. In agreement with our previous conclusion, the conductance change thus results from a conformational change following the protonation step. A model must therefore include a minimum of 4 states, in which protonation can occur in both conductance states, and in which the conductance change itself is possible in the unprotonated or protonated channel. An important



connotation of this model is the consideration of the low conductance conformation as an intrinsic property of the channel. The model can indeed simulate our data if  $k_2 < k_3$  and  $k_{-3} < k_{-2}$ . We have shown that the stability of the low conductance conformation depends on the type and concentration of permeant ion. Accordingly, the results with different permeant ions can be reproduced by changing in the model from one ion to the other only the rate constants of the transitions from the low to the high conductance states,  $k_{-2}$  and  $k_{-3}$ .

**Th-AM-C7 EFFECTS OF CA-CHANNEL AGONIST-ANTAGONIST ENANTIOMERS OF DIHYDROPYRIDINE 202-791 ON INSULIN RELEASE, CA UPTAKE AND ELECTRICAL ACTIVITY IN ISOLATED PANCREATIC ISLETS.** Boscherio, A.C., Carroll, P., De Souza, C. and Atwater, I. LCBG, NIDDK, NIH, Bethesda, MD.

Ca-channels in the B-cell membrane link the glucose-induced depolarization to insulin release. The + and - forms of the dihydropyridine, 202-791 (Sandoz), which acts as a Ca-channel agonist or antagonist, were studied using collagenase isolated rat islets to measure Ca uptake and insulin release and micro-dissected mouse islets to measure membrane potential. Glucose induced insulin secretion and Ca uptake were inhibited about 50% by the antagonist, (-)202 (10 or 100  $\mu$ M), while K induced insulin release and Ca uptake were inhibited 100% (10  $\mu$ M). Addition of the agonist, (+)202 (10  $\mu$ M) enhanced insulin release and Ca uptake over basal levels, but failed to further increase the glucose induced insulin release or Ca uptake. The (-)202 form was a stronger antagonist to the (+)202 form than was nifedipine. The effects of the (+) and (-) forms of 202-791 on the membrane potential and electrical activity were complex (similar to the effects of BAY K 8644 to inhibit and nifedipine to stimulate) illustrating the close association of K channel activation with Ca currents in the B-cell. In the presence of a K channel blocker, TEA, (+)202 increased and (-)202 decreased the duration of the action potentials. The results confirm the existence of a dihydropyridine sensitive Ca channel in B-cells and indicate the presence of another Ca channel which is insensitive to dihydropyridines and is perhaps activated by glucose.

**Th-AM-C8 MODE II CONDUCTION IN SINGLE Ca CHANNELS 10 mM Ca.** M. Mazzanti and L. J. DeFelice, Department of Anatomy and Cell Biology, Emory University, Atlanta, GA, 30322.

Hess et al. (Nature 311:538, 1984) in heart and Nowicky et al. (PNAS 82:2178, 1984) in nerve defined three types of Ca channel gating in 110 mM Ba: mode 0 (channel unavailability), mode I (brief openings), and mode II (long-lasting openings with very brief closings). In the absence of drugs, mode II is rare but may contribute significantly to overall current because of the long open times. We have studied the contribution of mode II conduction to the total Ca current while recording action potentials and patch currents simultaneously. In spontaneously beating 7d chick ventricle, with 1.5 mM Ca in the bath and 10 Ca in the pipette, we observe two kinds of openings: rare ones that last the duration of the action potential and common ones that are open primarily during the first 50 msec of the action potential. We tentatively associate these two types with mode II and mode I conduction. We plot individual openings vs. action potentials to measure instantaneous  $i(V)$  curves, and we average all openings over hundreds of beats to measure  $\langle i(V) \rangle$ . We compared curves in 10 Ca to those obtained in 10 Ba. Mode II  $i(V)$  curves are very similar in Ca and Ba except for magnitude. Mode II  $\langle i(V) \rangle$  curves, on the other hand, are totally different: the average Ba current peaks near -10 mV, while the average Ca current peaks near 40 mV and is zero between -80 and 0 mV. These differences are the result of nearly 100% mode II conduction when the Ca channel carries Ba but about 1% mode II conduction when the channel carries Ca. In spite of its rarity, mode II contributes significantly to the total Ca current during the plateau of the action potential, especially where the probability of mode I conduction is low but the driving force for Ca current is large. (Supported by NIH grant HL27385)

**Th-AM-C9 BLOCKING ACTIONS OF TRIVALENT LANTHANIDE CATIONS ON SINGLE DIHYDROPYRIDINE-SENSITIVE CALCIUM CHANNELS IN SKELETAL MUSCLE CELLS FROM THE MOUSE C2 CELL LINE.**

Jeffry B. Lansman, Dept. of Pharmacology, School of Medicine, University of California, San Francisco CA 94143.

The blocking actions of the trivalent lanthanide cations, La, Ce, Nd, Gd, Dy, and Yb, on unitary calcium channel currents were recorded from cell-attached patches on C2 myotubes with 110 mM  $\text{BaCl}_2$  in the patch pipet. In the presence of the dihydropyridine agonist (+)-202-791 which prolonged channel openings, block was resolved as discrete interruptions of the unitary current that could be described with a simple open channel block mechanism: single exponentials fitted histograms of open and blocked times; mean open times depended inversely on blocker concentration; mean blocked times were insensitive to blocker concentration. Exit rates (1/mean blocked time) for all lanthanide ions tested increased strongly as the membrane potential was hyperpolarized ( $\sim e$ -fold/23 mV), while entry rates (1/mean open time) were relatively insensitive to membrane potential. Individual lanthanide ions differed in both how fast they entered and exited the channel: entry rates decreased monotonically with 1/ionic radius -  $\text{La} (\sim 14 \times 10^6 \text{ M}^{-1}\text{s}^{-1}) > \text{Ce} > \text{Nd} > \text{Gd} > \text{Dy} > \text{Yb} (\sim 9 \times 10^4 \text{ M}^{-1}\text{s}^{-1})$ . Exit rates also decreased as 1/ionic radius but the decrease was less pronounced between Nd and Yb with La ( $\sim 200 \text{ s}^{-1}$  at 0 mV)  $> \text{Ce} > \text{Nd} > \text{Gd} (\sim 30 \text{ s}^{-1}) \sim \text{Dy} \sim \text{Yb} (\sim 20 \text{ s}^{-1})$ . The apparent affinity measured as the ratio entry rate/exit rate was similar for La, Ce, and Nd but decreased through Gd, Dy, and Yb reflecting the slower rate of entry of these ions. The results confirm the idea that the smaller ions enter the pore more slowly, presumably because they dehydrate more slowly;

5  $\mu\text{M}$   $\text{La}^{3+}$

1 pA  
80 ms

25  $\mu\text{M}$   $\text{Gd}^{3+}$

HP = -70 mV, TP = 0 mV

smaller ions also bind more tightly to the intra-pore site, but cation affinity for the binding site appears to reach a maximum for lanthanides with atomic radii between 0.93 to 0.97 angstroms.

**Tb-AM-C10** EFFECT OF INTERNAL NA IONS ON THE OUTWARD CURRENT THROUGH THE CA CHANNELS IN MOUSE NEOPLASTIC B LYMPHOCYTES. N. Yamashita, S. Ciani and S. Hagiwara, Dept. Physiol. BRI;JLNRC Univ. of Calif. Los Angeles, CA90024

Monovalent cations can carry the outward current through the Ca channels when the membrane potential is stepped to large positive levels. In mouse neoplastic B lymphocytes, type I Ca channels are the only voltage-gated channels present, allowing one thus to analyze the outward current through these channels in detail. Using the whole cell clamp configuration, the effect of monovalent cations on the outward current was analyzed by partly replacing Na in the pipette, [Na]<sub>i</sub>, with impermeant N-methyl-D-glucamine. The standard internal solution contained 156 mM Na and no other permeant cations. The external medium contained 2.5 mM Ca and 135 mM Na throughout. The reversal potential depended on [Na]<sub>i</sub> and the relation could be fitted with the constant field equation. However, other properties of the outward current were inconsistent with the predictions by that equation; (1) the amplitude of the outward current was much greater than expected. (2) the removal of the external Na had little effect both on reversal potential and the amplitude of the outward current. (3) the amplitude of the outward current at similar voltage had a steep dependence on [Na]<sub>i</sub>. These results could be fitted to a two-site, two-ion Eyring model in which double occupancy of the channel by Na is allowed in conjunction with double occupancy by Ca and mixed ions.



**Th-AM-D1 INHIBITION OF ALANINE RACEMASE BY ALANINE PHOSPHONATE: DETECTION OF AN IMINE LINKAGE TO PYRIDOXAL-5'-PHOSPHATE IN THE ENZYME-INHIBITOR COMPLEX BY SOLID-STATE  $^{15}\text{N}$  NUCLEAR MAGNETIC RESONANCE**, Valérie Copié<sup>a</sup>, W. Stephen Faraci<sup>a</sup>, Christopher T. Walsh<sup>a</sup>, and Robert G. Griffin<sup>a</sup>, Francis Bitter National Magnet Laboratory and Departments of Chemistry and Biology Massachusetts Institute of Technology Cambridge, MA 02139

Inhibition of alanine racemase from the gram-positive bacterium, *Bacillus stearothermophilus*, by 1-aminoethylphosphonic acid (Ala-P) proceeds via a two-step reaction pathway in which reactivation occurs very slowly. In order to determine the mechanism of inhibition we have recorded low-temperature, solid state  $^{15}\text{N}$ -NMR spectra from microcrystals of the  $^{15}\text{N}$ -Ala-P-enzyme complex, together with spectra of a series of model compounds which provide the requisite database for the interpretation of the  $^{15}\text{N}$  chemical shifts. Proton-decoupled spectra of the microcrystals exhibit a line at  $\sim 150$  ppm, which conclusively demonstrates the presence of a protonated Ala-P-PLP aldimine, and thus clarifies the structure of the enzyme-inhibitor complex. We also report the pH dependence of Ala-P binding to alanine racemase.

**Th-AM-D2 INTRAMOLECULAR ELECTRON TRANSFER BETWEEN THE REDOX COFACTORS OF XANTHINE DEHYDROGENASE.** M.C. Walker, D.E. Edmondson\* and G. Tollin, Department of Biochemistry, University of Arizona, Tucson, Arizona 85721 and \*Department of Biochemistry, Emory University School of Medicine, Atlanta, Georgia, 30322.

The rate constant for  $e^-$  transfer between the redox cofactors of xanthine dehydrogenase (XDH) have been measured using laser flash photolysis. The enzyme was reduced by one electron via the oxidation of 5-deazariboflavin radical, generated by the laser pulse. Only the transient for the decay of the deazaflavin radical showed a dependence on enzyme concentration ( $k = 0.7 \pm 0.1 \times 10^8 \text{ M}^{-1}\text{s}^{-1}$ ). From this observation, it was concluded that the molybdenum cofactor is the site for  $e^-$  donation from deazaflavin radical to the enzyme. Reduction of the two Fe/S centers in the enzyme displayed biphasic kinetics ( $k_1 = 110 \pm 13 \text{ s}^{-1}$ ,  $k_2 = 8 \pm 2 \text{ s}^{-1}$ ). The FAD cofactor underwent rapid reduction to the semiquinone ( $k = 1600 \pm 200 \text{ s}^{-1}$ ), followed by slower reoxidation ( $k = 79 \pm 5 \text{ s}^{-1}$ ). Reduction by XDH by methyl viologen radical ( $\text{MV}^\cdot$ ), generated by *in situ* electron transfer from deazaflavin radical, was observed to proceed via direct interaction with the Fe/S centers ( $k = 6.7 \pm 0.5 \times 10^8 \text{ M}^{-1}\text{s}^{-1}$ ). Alkylation of the FAD in XDH with iodoacetamide had no effect on enzyme reduction by  $\text{MV}^\cdot$ . Comparison of these results with those obtained for xanthine oxidase [cf. Edmondson, et al., in *Flavins and Flavoproteins*, 403-408 (1987)] suggest that the FAD of XDH is less accessible. Supported by NIH grant DK15057.

**Th-AM-D3 PHOSPHORYLATIVE MODIFICATION OF THE  $\text{Mg}^{2+}$ -ATPase ASSOCIATED WITH RAT CARDIAC NUCLEI.** R.C. Gupta\*, E.F. Young\*, D.G. Ferguson\*, and E.G. Kranias\*, Departments of Pharmacology & Cell Biophysics\*, and Physiology & Biophysics\*, University of Cincinnati, Cincinnati, Ohio 45267-0575.

Phospholamban (PLB), the putative regulator of the  $\text{Ca}^{2+}$ -ATPase in cardiac sarcoplasmic reticulum (SR), is not only present in SR but it is also abundant and evenly distributed in the outer nuclear envelope of myocardial cells. To study the role of PLB in the nucleus, nuclei were purified essentially devoid of SR contamination, from rat ventricles. Freshly isolated nuclei possessed a  $\text{Mg}^{2+}$ -dependent ATPase activity of  $30 \mu\text{mol Pi/mg/h}$ . Phosphorylation of nuclei in the presence of  $10 \mu\text{M}$  ATP and  $5 \text{ mM}$   $\text{MgCl}_2$  occurred predominantly on a  $55,000 \text{ Mr}$  protein and was associated with a significant decrease in the  $\text{Mg}^{2+}$ -ATPase activity. Inclusion of the catalytic subunit of cAMP-dependent protein kinase did not further stimulate the phosphorylation of the  $55 \text{ Kda}$  protein but it resulted in phosphorylation of a  $125$ ,  $43$ ,  $30$ ,  $27$ , and  $11.5 \text{ Kda}$  proteins. The  $27 \text{ Kda}$  phosphoprotein exhibited the characteristic mobility shift of PLB and it could be converted to an  $11.5 \text{ Kda}$  phosphoprotein upon boiling in SDS. However, additional phosphorylation by the catalytic subunit had no further effect on the  $\text{Mg}^{2+}$ -ATPase activity. These results indicate that a protein with  $\text{Mr } 55,000$  may be involved in modulating the  $\text{Mg}^{2+}$ -ATPase activity in cardiac nuclei. (Supported by NIH grants HL26057, HL22619, and HL34979.)

**Th-AM-D4 QUATERNARY STRUCTURE OF SINGLE SITE MUTANTS OF *E. COLI* ASPARTATE TRANSCARBAMOYLASE.**

D.S. Burz and N.M. Allewell, Wesleyan University, Middletown, CT 06457.

Analytical gel chromatography has been used to monitor the changes in quaternary structure associated with binding of the bisubstrate analog PALA (N-phosphonacetyl-L-aspartate) and to examine the quaternary structure of several single site mutants. The transition from the T to the R state induced by binding of PALA has previously been shown to reduce  $s_{20,w}$  by 3.3% (Howlett, G.J. and Schachman, H.K. (1977) *Biochemistry* 16, 5077-83) and to increase the radius of gyration by 2.4 Å (Moody, M.F. *et al.* (1979) *J. Mol. Biol.* 133, 517-32). We have found that the partition coefficient on Sephacryl S-400 in 0.04M  $\text{KH}_2\text{PO}_4$ - $\text{K}_2\text{HPO}_4$ , 0.2mM EDTA, 0.2mM DTT, pH 8.3, 5°C decreases by 3% in the presence of saturating PALA as a result of a change in the radius of gyration from 63.5 Å to 65.9 Å. Partition coefficients of several mutant proteins with single site mutations in the c chain (Glu->Gln 50, Asp->Gly 100, Lys->Ile 164, Tyr->Phe 165, Glu->Ser 234, Glu->Ala 239, Glu->Gln 239, Tyr->Phe 240, Arg->Gly 269) in the absence of PALA differ from that of the wild type enzyme by  $\pm 0.5\%$ . Mutations which are not at intersubunit interfaces appear to have no effect on quaternary structure. The 0.4% change in the partition coefficient of mutant Tyr->Phe 165 is consistent with the suggestion based on activity measurements that this protein is locked in the T state (Wales, M.E. *et al.* (1988) *J. Biol. Chem.* 263, 504-9). Similarly the -0.5% change in the partition coefficient of mutant Glu->Gln 239 supports the conclusion drawn from activity and x-ray scattering measurements that the quaternary structure of this mutant is shifted towards the R state (Ladjimi, M.M. and Kantrowitz, E.R. (1988) *Biochemistry* 27, 276-83); however this shift is apparently not complete. Supported by NIH grant AM-17335.

**Th-AM-D5 ACTIVITY OF GLUCOCEREBROSIDASE IN MIXED MICELLES WITH LIPID-SOLUBLE AND WATER-SOLUBLE FLUOROGENIC SUBSTRATES** T. C. Richards\*, A. S. Waggoner\*, and R. H. Glew# Department of Biological Sciences, Carnegie Mellon University\*, Pittsburgh PA 15213 and Department of Biochemistry, University of Pittsburgh School of Medicine#, Pittsburgh PA 15261

The rate of hydrolysis of fluorogenic substrate analogs by glucocerebrosidase (M-G) in a mixed micelle system depends strongly on the length of alkyl chains on the substrates. The seven analogs of 4-alkyl umbelliferyl-β-D-glucoside (UGn) used in this study are designated UG1, UG3, UG5, UG7, UG9, UG11, and UG17 where n indicates the number of carbon atoms in the aliphatic chain at the 4-position of the chromophore. UG1 is a water-soluble fluorogenic substrate commonly used in M-G assays. Lineweaver-Burk analyses of the M-G assays were done to obtain kinetic constants. We have shown that the lipid analogs of UG1 are better for assaying M-G because apparent  $K_m$ 's are lower and enzyme activities are higher. The apparent  $K_m$ 's decrease up to UG5, then they decrease slightly or stay the same. Fluorescence polarization of the substrates was measured to determine partition coefficients of substrates in mixed micelles. The binding of the substrates to micelles increases as the alkyl chain-length increases. UG7 to UG17 are completely bound in 1% Lubrol:0.6% taurocholate mixed micelles. The apparent  $K_m$  depends on both the amount of substrate bound to the micelle and some property of the enzyme's binding site that is sensitive to the alkyl region of the substrate.  $V_{max}$  does not vary significantly as substrate chain length increases. UG11 was a gift from Dr. G. Legler, Institut für Biochemie der Universität zu Köln, Köln FRG. Supported by grant GM34639.

**Th-AM-D6 KINETIC EVIDENCE FOR MALONYL-CoA SENSITIVE AND MALONYL-CoA INSENSITIVE FORMS OF OVERT CARNITINE PALMITOYLTRANSFERASE (CPT-I) IN CANINE HEART MITOCHONDRIA.** Daniel F. Pauly, Division of Cardiovascular Disease, Univ. of Alabama at Birmingham, Birmingham, Alabama 35294.

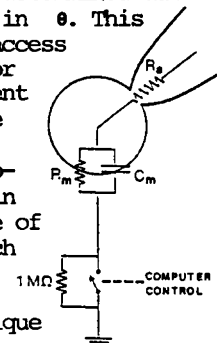
Malonyl-CoA inhibits CPT-I activity competitively but not completely, prompting some to call the kinetics complex. Here two kinetic models are tested to explain this partial inhibition. In a one enzyme model, inhibition is partial when an ESI complex can produce product (Segel, *Enzyme Kinetics*, Wiley, 1975). The velocity is defined by eqn. 1, where  $\alpha > 1$  reflects on the stability of the ternary complex. Alternatively a two enzyme model is possible where two forms of the enzyme are present: one that is inhibitable and one that is not (eqn. 2). In 4 preparations of isolated canine heart mitochondria CPT-I activity was measured at each of 6 malonyl-CoA concentrations and 7 palmitoyl-CoA concentrations using an isotope forward assay. The kinetic data were fit to these two models and statistically compared to the model for simple competitive inhibition. The one enzyme model shows a lower average error sum of squares (ESS) (5.2) than the simple competitive model (5.8), reaching statistical significance in 1 of 4 experiments as well as overall ( $p < 1 \times 10^{-2}$ ). The two enzyme model however gives even lower ESS (4.3), reaches greater significance overall ( $p < 1 \times 10^{-7}$ ), and is significant in all 4 experiments individually. This better kinetic fit suggests the presence of two forms of overt CPT in canine heart mitochondria: one that is inhibitable by malonyl-CoA and one that is not. A malonyl-CoA regulatory protein has been suggested by others and the two forms postulated may reflect the catalytic subunit with and without this regulatory subunit. Supported by NIH HL 38863.

$$\text{eqn. 1} \\ v = \frac{v_{max} [S]}{K_s \left( 1 + \frac{[I]}{K_i} \right) + [S]} \\ \text{eqn. 2} \\ v = \frac{v_{max1} [S]}{K_{s1} \left( 1 + \frac{[I]}{K_{i1}} \right) + [S]} + \frac{v_{max2} [S]}{K_{s2} + [S]}$$

**Th-AM-E1 PHASE TRACKING: A NEW TECHNIQUE FOR CELL MEMBRANE CAPACITANCE MEASUREMENTS**

N. Fidler and J. M. Fernandez. U. of Pennsylvania, Phila., PA, 19104.

Measurement of the membrane capacitance of a cell is used as an assay for exocytosis in single cells. We measure changes in membrane capacitance ( $C_m$ ) of mast cells using a software based phase detector (Joshi & Fernandez (1988) *Biophys. J.* 53: 885-892). We have developed a technique which allows accurate on line determination of the phase angle,  $\theta$ , at which to measure the capacitance signal, which is based solely on the cell's electrical parameters irrespective of the capacity compensation of the patch clamp amplifier. Moreover,  $\theta$  can be rapidly and frequently determined during a  $C_m$  measurement so that the phase detector can follow the changes that occur in  $\theta$ . This phase tracking technique involves creating resistance changes in series with the access resistance to the cell, by a computer controlled switch which shorts a  $1\text{M}\Omega$  resistor at the ground input of the amplifier (Fig). This determines the phase of the current vector associated with changes in  $R_a$ . To measure the capacitance signal, the phase detector is then simply aligned perpendicular to this vector. We have tested the phase tracking technique using an RC series circuit to simulate the electrical properties of a cell ( $C_m$  and  $R_a$ ). For a 4-fold increase in  $C_m$  and a 4-fold decrease in  $R_a$ , the value of  $\theta$  found by this technique followed precisely the predicted change of the phase angle calculated from impedance analysis of the model cell. This approach effectively eliminated the error in measuring the magnitude of small step changes in  $C_m$ . We have also demonstrated the usefulness of this technique in following real  $C_m$  changes in degranulating mast cells. In summary, the phase tracking technique allows error free  $C_m$  measurements to be made throughout an entire degranulation.

**Th-AM-E2 SURFACE DIELECTRIC CONSTANT, HYDROPHOBICITY AND MEMBRANE FUSION.**

S. Ohki and K. Arnold, Department of Biophysical Sciences, School of Medicine, State University of New York at Buffalo, Buffalo, N.Y. 14214

Membrane fusion and its associated membranes properties were examined. In addition to the interfacial tension of membranes, the surface dielectric constant of the membrane was found to correlate well with the extent of membrane fusion. The increase in interfacial tension of the membrane and the decrease in dielectric constant of the membrane surface polar region are both related to the increase in hydrophobicity and the reduction of hydration energy of the membrane surface. The points mentioned above were demonstrated by experiments using acidic and neutral phospholipid membranes as a function of various cation concentrations. The surface dielectric constants of the membranes were deduced from the experimental results obtained by a fluorescent method. Both the increase in hydrophobicity and the decrease in hydration energy of the membrane surface together with the reduction of electrostatic interaction energy allow the two interacting membranes to come to a close contact (molecular contact of membranes) which may initiate membrane fusion. (Supported by a grant from NIH-GM 24840).

**Th-AM-E3 PURE LIPID VESICLES CAN INDUCE CHANNEL-LIKE CONDUCTANCE STEPS IN PLANAR MEMBRANES.**  
Dixon J. Woodbury. Graduate Department of Biochemistry, Brandeis University, Waltham, Massachusetts 02254.

Planar lipid bilayers were observed to exhibit "typical channel behavior" following brief exposure to large concentrations of lipid vesicles devoid of protein. Vesicles, formed by sonication of lipids suspended in aqueous buffer, were ejected  $\sim 0.5$  nm from a planar bilayer with a small pipet. Over the next several minutes the bilayer conductance changed in ways usually considered to be indicative of reconstituted protein channels including: step conductance changes (both up and down), inactivation, flickering, and ion selectivity. Conductance steps ranged from 50-1000 pS (20 mV holding voltage). Typically, conductance jumps started 30 seconds after vesicle addition, peaked after two minutes, and the membrane conductance returned to baseline by five minutes. This observation demonstrates the need for caution in interpreting conductance changes which occur following ejection of channel-containing vesicles near the bilayer. (Supported by a fellowship from MDA.)

**Th-AM-E4** INHIBITION OF CHROMAFFIN CELL EXOCYTOSIS BY A SPECIFIC ANTIBODY IS REVEALED BY CAPACITANCE MEASUREMENTS. F.E. Schweizer, R.J. Bookman\*, T. Schäfer, and M.M. Burger. Friedrich Miescher Institut, Basel, Switzerland, and \*Howard Hughes Medical Institute, Department of Physiology, University of Pennsylvania, Philadelphia, Pennsylvania.

The molecular machinery responsible for exocytosis is largely unknown. Proteins which bind to secretory vesicles are likely candidates and one example is a protein isolated from chromaffin cell plasma membranes on the basis of its specific and strong binding to chromaffin granules (Meyer & Burger, J.B.C., 254, 1979). This Chromaffin Granule Binding Protein (CGBP) shows Ca-independent binding to granules and no binding to mitochondria or lysosomes. Antisera raised against purified CGBP detected a single protein of MW 51kD on immunoblots of plasma membranes but not granule membranes. The localization to the plasma membrane and the binding to granules suggested that CGBP plays a role in 'docking' of granules to the plasma membrane prior to their fusion (Schäfer et al., Biosci.Rep., 7, 1987). We tested this idea directly by introducing antibodies against CGBP into the cytoplasm and measured the effect on secretory activity by monitoring changes in membrane capacitance using whole-cell techniques. Diffusion into cytoplasm was controlled by including a fluorescently-labeled, non-specific Ab in the patch pipette.  $\text{Ca}^{++}$  influx and exocytosis were stimulated by depolarizing pulses from -75mV to +20mV. Cells loaded with a non-specific Ab against plasma membrane showed capacitance jumps in response to 100ms pulses. 7 out of 9 cells loaded with specific anti-CGBP Abs showed no capacitance jumps even in response to longer depolarizations and despite the fact that the  $\text{Ca}^{++}$  current was not blocked. Thus anti-CGBP inhibits exocytosis in chromaffin cells, indicating a functional role for CGBP in the exocytotic machinery.

**Th-AM-E5** DEHYDRATION IN THE PROCESS OF MEMBRANE FUSION AS EVIDENCED BY ANS FLUORESCENCE.

K.C.Lin and L.Y.Song, Department of Biophysics, Beijing Medical University, Beijing, China.

Membrane fusion involves several stages in which the close contact of two opposing membranes is a necessary step. Since cells are surrounded by water in a more or less ordered form which offers a repelling force between cell membranes to prevent the close contact of them. Therefore it is evident that in order to fuse two cells together, the removal of water, i.e. dehydration is necessary and common to all kinds of fusion, whether it is induced by chemicals, virus, cations or electric fields. Experimental evidences have been given in this work by the fluorescence changes of ANS, a fluorescence probe labelled on membrane, the fluorescence characteristics are sensitive to the microenvironment: blue shift of fluorescence peak and quantum yield increase will occur as the polarity decreases. By this method, fusion of negatively charged liposomes induced by  $\text{Ca}^{2+}$  and  $\text{H}^+$ , erythrocyte ghosts by calcium phosphate as well as by electrofusion had been monitored. In all these processes blue shift and quantum yield increase could be seen, implying that the removal of water (dehydration) may be a first step in the fusion process.

**Th-AM-E6** pH-DEPENDENT FUSION OF RECONSTITUTED VESICULAR STOMATITIS VIRUS ENVELOPES WITH VERO CELLS: MEASUREMENT BY DEQUENCHING OF FLUORESCENCE. Marie-Therese Paternostre, R. Joel Lowy, and Robert Blumenthal, (Intr. by R.J. Turner), LTB, NCI and LKEM, NHLBI, NIH, Bethesda, Md. 20892.

We have reconstituted membranes of Vesicular Stomatitis Virus (VSV) after solubilization of the viral envelope with Triton X100. The detergent was removed by direct addition of SM2 biobeads without loss of viral protein. The resulting virosomes were homogeneous in composition according to sucrose gradient centrifugation with 80% of lipids associated with 80% of protein in the same band. Low light level video microscopy indicated that the virosome size was inhomogeneous with sizes ranging from that of single virions to large aggregates. Removal of large aggregates by passage through a millipore filter resulted in better fusion activity. Fusion of the virosomes with Vero was cells observed by fluorescence microscopy using both a lipid probe incorporated into the virosome bilayer, and an aqueous probe incorporated into its aqueous space. The kinetics of fusion was monitored spectrofluorometrically with virosomes containing the lipid probe. Fusion at the plasma membrane began immediately after lowering the pH below 6.5, and showed an approximately exponential time course. The pH profile of reconstituted VSV fusion was similar to that of the intact virus. Control virosomes, which had been exposed to 56 °C for 15 min, did not show pH-dependent fluorescent changes.

**Th-AM-E7 SIALOGLYCOPROTEIN OF VESICULAR STOMATITIS VIRUS: ROLE OF NEURAMINIC ACID IN VIRUS-CELL FUSION.** Anu Puri, Settimio Grimaldi and Robert Blumenthal. Section on Membrane Structure and Function, LTB, NCI, NIH, Bethesda, Md. 20892

Treatment of Vesicular Stomatitis Virus (VSV) with Neuraminidase free of proteolytic activity did not affect binding to Vero cells, but significantly enhanced the rate of fusion of the viral membrane with the plasma membrane of the cells. The fusion was measured using an assay for lipid mixing based on the relief of self-quenching of octadecylrhodamine (R18) fluorescence. The pH-dependence of fusion of neuraminidase-treated virus was similar to that seen with untreated virus. Incubation of untreated or neuraminidase-treated VSV with mixed gangliosides resulted in a reduction of the fusion activity. Measurement of fluorescence energy transfer in dansyl-labeled virus indicated that treatment with neuraminidase alters the conformation of the sialoglycoprotein to a state which might more readily mediate pH-dependent fusion.

**Th-AM-E8 INTERDIGITATED LIPID MECHANISM FOR CELL MEMBRANE FUSION.** *Stephanie Tristram-Nagle and John F. Nagle*, Depts. Biological Sciences and Physics, Carnegie Mellon University, Pittsburgh, PA 15208.

An hypothesis is presented for the molecular mechanism of cell membrane fusion such as occurs during exocytosis, endocytosis and infection of cells by enveloped viruses. The core of the hypothesis is that a central step in fusion consists of acyl chain interdigitation of phospholipids in two closely apposed bilayers. This step, coupled with lateral diffusion of lipids from the interdigitated fusion line to the unapposed regions of both membranes, provides a mechanism with small energy barriers that thins the original membrane pair to one membrane with roughly one quarter the original thickness. Subsequent rupture of the single membrane, particularly at the joints connecting it to the original bilayers, then results in fusion. This hypothesis is consistent with, and indeed was suggested by, electron micrographs published by Palade and Bruns (*J. Cell. Biol.* 37:633-649 (1968)). This hypothesis is also supported by observations that fusogenic substances such as acetylcholine, chlorpromazine, tetracaine, glycerol and ethylene glycol also trigger transformations from normal bilayers to interdigitated bilayers in model lipid systems. The chemical structures of one class of interdigitators are similar to many positively charged amine secretagogues, and we suggest that the high concentration of secretagogues inside vesicles (0.7 M) may enhance membrane fusion by interdigitation of the lipid acyl chains of intracellular vesicles. The roles of different lipids, such as phosphatidylinositol, phosphatidylserine and cholesterol, are discussed.

**Th-AM-E9 EXOCYTOSIS IN GTP $\gamma$ S STIMULATED MAST CELLS OCCURS IN SEQUENTIAL MODE.** Guillermo Alvarez de Toledo & Julio. M. Fernandez. University of Pennsylvania. Philadelphia, PA 19104-6085

We have studied individual exocytotic events in degranulating murine mast cells, by monitoring the cell membrane capacitance. The cell membrane capacitance was determined using the patch clamp technique and a software based phase detector. Exocytosis was induced by intracellular perfusion with GTP $\gamma$ S (1-10  $\mu$ M). The capacitance step amplitude histograms showed a significant number of very large granule surface areas compared to the ones predicted by electron microscopy studies. We have developed a computer model to test the hypothesis whether these large granules are the result of normal granulogenesis or they are formed by granule to granule fusion prior to exocytosis (compound exocytosis). The model was constructed using a tridimensional matrix where each element corresponds to a secretory granule (assigned 0), except the outer layer of the matrix, which corresponds to plasma membrane (assigned 1). The rules assigned to simulate compound exocytosis were such that a randomly selected granule could fuse either to a neighbor or the plasma membrane. Once a granule(s) fused with the membrane its value was set to 1 and computed as a capacitance step. The model was well behaved since it accurately reproduced the time course of capacitance increases measured in real cells as well as the latency times between successive fusions. In real data, large steps appeared mostly at the beginning of the degranulation, whereas in the model they appeared mainly in the middle and the end of the simulation. These results suggest that large secretory granules pre-existed stimulation and once the stimulus triggers exocytosis there is no fusion of granules among themselves unless one of the previous granules has already fused with the membrane. This also may indicate that the fusogenic agent is membrane bound rather than dissolved in the cytoplasm.

**Th-AM-E10** VIDEO MICROSCOPY STUDIES OF VIRUS-MEMBRANE INTERACTIONS. W.D. Niles, M.E. Peeples, F.S. Cohen. Rush Medical College, Chicago, IL 60612.

We are using video fluorescence and transmission microscopy to develop methods to study the mechanisms by which the spike proteins of enveloped viruses mediate membrane binding and fusion. As a first step, we have compared the abilities of Sendai and influenza strain PR8 virions to bind to planar phospholipid bilayer membranes and to lyse human red cells. Influenza virions were brightly labelled with the fluorescent dye octadecyl rhodamine. Virions were readily apparent when bound to planar membranes and viewed with a SIT camera. The amount of virus binding depended on the ganglioside (G<sub>D1a</sub> and G<sub>T1b</sub>) content of the planar membrane.

Influenza also promoted the adsorption of red cells to ganglioside-containing planar membranes, and hemolysis occurred when the pH was lowered. Viewing virus-induced hemolysis on a glass slide by bright-field microscopy enabled determination of the rate of red cell lysis as a function of pH at the level of individual red cells. Unlabelled influenza virus quickly induced the lysis of red cells at 33° C after the pH of the medium was lowered from 7.4 to < 5.0. In contrast, Sendai virions were less bright when labelled with octadecyl rhodamine and the extent of labelling varied. The magnitude of Sendai binding to planar membranes and its dependence on ganglioside content also showed greater variability. Although unlabelled Sendai promoted the binding of vesicles, loaded with the fluorescent dye calcein, to planar membranes, the virus did not cause the release of dye from the vesicles and, therefore, did not promote fusion. Finally, the rate of Sendai-induced hemolysis at pH 7.4 and 33° C was about 1/5 of that for influenza virus at pH 5.0. We conclude that influenza is the better virus for study in the model system due to its brightness when fluorescently labelled and its greater rate of fusion as measured by hemolysis. Supported by NIH grants GM27367 and AI21924.

**Th-AM-F1** CHLORIDE TRANSPORT MEASURED IN CULTURES OF CANINE TRACHEAL EPITHELIAL CELLS USING AN EN-TRAPPED FLUORESCENT INDICATOR. A.C. Chao, M.C. Sellers, J.H. Widdicombe and A.S. Verkman. Cardiovascular Research Institute, University of California, San Francisco, CA 94143.

An optical method for continuously monitoring intracellular Cl activity in cultured epithelial cells has been developed to examine the mechanisms and regulation of Cl transport. Primary cultures of canine tracheal cells were grown to confluency on thin glass cover slips and on porous filters. Short circuit current ( $2\text{--}10 \mu\text{A}/\text{cm}^2$ ), representing apical Cl channel activity, increased >5-fold in response to serosal isoproterenol addition ( $10 \mu\text{M}$ ). Cells made transiently permeable in hypotonic solution were loaded with the Cl-sensitive fluorophore 6-methoxy-N-(3-sulfoethyl) quinolinium (SPQ) ( $5 \text{ mM}$ ,  $4 \text{ min}$ ,  $150 \text{ mOsm}$ ). Intracellular SPQ fluorescence was monitored continuously by epifluorescence microscopy (excitation  $355 \pm 5 \text{ nm}$ , emission  $>410 \text{ nm}$ ) without photobleaching. SPQ leakage from the cells was  $<10\%$  in  $60 \text{ min}$  at  $37^\circ\text{C}$ . Intracellular calibration of SPQ fluorescence vs [Cl] ( $0\text{--}80 \text{ mM}$ ) was carried out using high-K buffers containing the ionophores nigericin ( $5 \mu\text{M}$ ) and tributyltin ( $10 \mu\text{M}$ ); SPQ fluorescence was quenched with a Stern-Volmer constant of  $15 \text{ M}^{-1}$ . Cl transport was measured in response to addition and removal of  $110 \text{ mM}$  Cl from the bathing solution. Addition of isoproterenol ( $10 \mu\text{M}$ ) gave a reversible, marked increase in Cl flux ( $5\text{--}10\text{-fold}$  increase in efflux rates); the increase was inhibited  $>50\%$  by the Cl-channel blocker diphenylamine-2-carboxylic acid ( $1 \text{ mM}$ ). In the absence of isoproterenol, removal of external Na or addition of furosemide ( $0.5 \text{ mM}$ ) reduced Cl flux by  $> 5\text{-fold}$ . These results establish an accurate, optical method for the real-time measurement of intracellular Cl level in intact cells. The results in tracheal epithelial cells demonstrate the presence of an isoproterenol-regulated Cl channel and a furosemide-sensitive Na-(K)-Cl coupled transport mechanism.

**Th-AM-F2** SPATIAL DISTRIBUTION OF CALCIUM IN ISOLATED RAT PAROTID ACINI FOLLOWING CHOLINERGIC STIMULATION. Steen Dissing, Birgitte Nauntofte, and Ove Sten-Knudsen, Institute of General Physiology and Biophysics, Panum Institute, University of Copenhagen, Denmark.

Concentrations of intracellular, free  $\text{Ca}$  ( $\text{Ca}_i$ ) following cholinergic stimulation were measured by digital image processing of individual fura-2 loaded rat parotid acini.  $\text{Ca}_i$  were determined by ratioing images (1 image/sec) obtained at  $338$  and  $380 \text{ nm}$  excitation from acini suspended in media thermostatically controlled at  $37^\circ\text{C}$  on a microscope stage. In a Krebs-Ringer buffer ( $1 \text{ mM } \text{Ca}_o$ ) carbachol causes a transient rise in  $\text{Ca}_i$  from  $150 \text{ nM}$  to approximately  $700 \text{ nM}$  at both the basolateral and luminal membranes with a peak value obtained  $1\text{--}2$  seconds after stimulation. Over the following  $45$  seconds  $\text{Ca}_i$  falls towards prestimulatory levels with a tendency to decrease at the fastest rate near the basolateral membranes. Simultaneously with the rise in  $\text{Ca}_i$  the acini shrink and approach a minimum volume  $15\text{--}20$  seconds after stimulation. When carbachol-stimulation occurs under conditions where the  $\text{Ca}$  distribution across the plasma membrane is close to the  $\text{Ca}$  equilibrium potential ( $10 \text{ nM } \text{Ca}_o$ ,  $150 \text{ nM } \text{Ca}_i$ ,  $-60 \text{ mV}$ ; Nauntofte & Dissing, *Am. J. Physiol.*, **253**, G290-G297, 1987)  $\text{Ca}_i$  first increases transiently followed by frequent bursts of short durations of  $< 1 \text{ sec}$ . Supported by I. & L. DANIN, NOVO, Haensch Foundations and the Danish Natural Research Council.

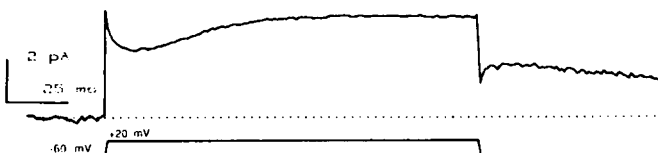
### Th-AM-F3 $\text{Ca}^{++}$ -CURRENT IN HUMAN EPIDERMAL CELLS

Etienne C. Reverdin, Gal A. Cohen, Nicholas M. Birchall<sup>†</sup> and Emile L. Boulpaep, Depts. of Cellular and Molecular Physiology & Dermatology<sup>†</sup>, Yale University School of Medicine, New Haven, CT 06510.

Cytoplasmic calcium has been demonstrated to be regulated in human keratinocytes. The rationale of our study is to investigate whether human keratinocytes regulate their calcium transport by means of ionic channels. With the patch-clamp technique we have demonstrated the existence of single-channel barium-ion currents through calcium-type channels in monolayers of normal and SV40-adenovirus transformed human keratinocytes. Bath solution contained (in mM):  $140 \text{ K-Aspartate}$ ,  $10 \text{ EGTA}$ ,  $10 \text{ Hepes}$  ( $\text{pH } 7.5$ ),  $10 \text{ Glucose}$ . Pipette solution contained:  $110 \text{ BaCl}_2$ ,  $\text{Hepes}$  (titrated to  $\text{pH } 7.35$  with  $\text{TEA-OH}$ ),  $10 \text{ Glucose}$ .

Firstly, using the transformed cell line, in the cell-attached configuration with  $0.005 \text{ mM}$  Bay-K8644 [Miles] in the pipette, we found inward-directed current rectifying at hyperpolarized patch-potentials (pipette positive to ground). The linear segment of the I-V relationship revealed a slope conductance of  $20 \text{ pS}$ . Inward-current channel openings were observed continuously at all patch-potentials between  $-60$  and  $+60 \text{ mV}$ . The extrapolated reversal potential was  $>> 60 \text{ mV}$ , confirming  $\text{Ba}^{++}$  as the current carrier through calcium channels.

Secondly, in subconfluent cultures of normal human keratinocytes grown in medium containing  $1.8 \text{ mM } \text{Ca}^{++}$ , depolarizing voltage pulses were applied to cell-attached patches.  $64$  pulses were applied before and after addition of  $0.005 \text{ mM}$  Bay-K8644 to the bath. The resulting whole-patch currents were averaged. The figure shows the extra current induced by Bay-K8644, obtained by digital subtraction of the control current.



The transient inward directed current which is observed at the beginning of the depolarizing step can only be carried by  $\text{Ba}^{++}$ -ions.

We conclude that the apical membrane of human keratinocytes contains  $\text{Ca}^{++}$ -channels which are activated by the dihydropyridine calcium channel agonist Bay-K8644.

**Th-AM-F4 IDENTIFICATION OF CELLS RESPONSIBLE FOR ACID AND ALKALI SECRETION IN THE TURTLE**

BLADDER. J.H. Durham, A. Shipley and Carl Scheffey. Mt. Sinai Sch. Med., N.Y., N.Y., Marine Biological Laboratories, Woods Hole, MA., and Dept. Biology, Columbia Univ., N.Y., N.Y.

The turtle urinary bladder contains two distinct cell types: the majority are granular (G) and the minority carbonic anhydrase rich (CA) cells. We applied the 2D-vibrating probe technique to rigorously determine the cell source(s) of electrogenic luminal acidification and alkalization. Bladders were mounted in an Ussing chamber apical side up under an upright microscope, the luminal surface viewed during perfusion and the short circuit current (Isc) measured under conditions producing acidification or alkalization current. The magnitude, direction and angles of the cell currents were determined by moving the probe across each cell and plotting them over the digitized image of the field of view. For acidification, in one representative experiment of 7, a minority of cells in the field of view were found to produce a mean ( $\pm$ SEM) point source current of  $120 \pm 0.01$  pA (positive charges flowing out of the cell) while the acidification Isc was  $7 \text{ ua/cm}^2$ . After inhibition of acidification, the Isc and cell currents decreased to zero levels. In 3 experiments, the same cells which had been found to be producing the acidification current were stained by Ag identifying them as CA cells. In other experiments, cAMP-induced alkalization current could not be localized over any particular cell, but those which had been determined to produce acidification current did not reverse to produce alkalization current. These data: 1) demonstrate that acidification is produced by CA cells and 2) indicate that cAMP-induced alkalization may be produced by the G cells. (Supported in parts by NIH R23DK35754 (to JHD) and the National Vibrating Probe Facility)

**Th-AM-F5 G-PROTEIN REGULATION OF A CATION CHANNEL IN RENAL EPITHELIAL CELLS.** D. Light, D. Ausiello and B. Stanton. Dept. of Physiol., Dartmouth Med Sch, Hanover, NH and Mass Gen Hosp, Boston, MA.

G-binding proteins transduce receptor-mediated signals for a number of effector systems. In particular, G-proteins couple receptors to  $\text{K}^+$  and  $\text{Ca}^{2+}$  channels in myocytes and directly regulate channel activity. In polarized epithelial cells, G-proteins are coupled with cell-surface receptors in the basolateral membrane whereas G-proteins located in the apical membrane may not be linked with receptors, but appear to modulate ion channels. We determined if a G-protein directly gates a cation channel in the apical membrane of rat inner medullary collecting duct (IMCD) cells. Patch clamp studies were conducted on inside-out patches of IMCD cells in primary culture. Previous studies showed that the cation channel is inhibited by amiloride and mediates electrogenic  $\text{Na}^+$  uptake (Light et al., *Am. J. Physiol.* 255:F278, 1988). GTPYS ( $10^{-4}$  M) in the bath increased the single channel open probability (Po) from 0.17 to 0.47 ( $n=9$ ;  $P<0.005$ ) in the absence of any other channel agonist. In contrast, GDP $\beta$ S ( $10^{-4}$  M) reduced Po from 0.55 to 0.25 ( $n=7$ ;  $P<0.02$ ). Activated pertussis toxin (PTX; 100 ng/ml) with  $\text{NAD}^+$  inhibited the channel: Po fell from 0.57 to 0 ( $n=9$ ;  $P<0.001$ ). In PTX-treated membrane patches, the  $\alpha_{i-3}$  subunit of  $\text{G}_i$  (2 pM to 400 pM) in the bath solution activated the channel. The properties of the  $\alpha_{i-3}$  activated channel were similar to cation channels in control patches. GTPYS ( $10^{-4}$  M;  $n=3$ ) also reversed the PTX-inactivation of the channel. Conclusion: a PTX-sensitive,  $\alpha_{i-3}$  protein in the apical membrane directly gates the cation channel. The  $\text{G}_i$  protein in the apical membrane may not be linked directly to a receptor, however,  $\text{G}_i$  may be regulated indirectly via a receptor coupled G-protein located in the basolateral membrane.

**Th-AM-F6 CONDUCTANCE PATHWAYS FOR  $\text{HCO}_3^-$  IN THE BASOLATERAL MEMBRANE OF INTESTINAL CELLS.** John F. White and Dorothy Ellingsen, Dept. of Physiology, Emory University, Atlanta, GA 30322.

In order to understand the mechanisms by which  $\text{HCO}_3^-$  ions exit across the basolateral membrane of Amphiuma small intestinal cells during active  $\text{H}^+$  secretion the influence of bath  $\text{HCO}_3^-$  on the enterocyte serosal membrane potential ( $v_s$ ) was measured using conventional microelectrodes. The villus sheet preparation was used in which the villus is transformed into a two-dimensional array of cells providing direct access to the basal membrane for microelectrode impalement. When tissues were incubated in  $\text{Cl}^-$ -free ( $\text{SO}_4^{2-}$ -based) medium  $v_s$  averaged  $-85.8 \pm 2.1$  mV. Elevation of serosal bath  $[\text{HCO}_3^-]$  at constant  $\text{CO}_2$  hyperpolarized the serosal membrane significantly ( $P<0.01$ )  $-7.5 \pm 1.7$  mV. Reduction of the  $[\text{HCO}_3^-]$  depolarized the membrane significantly ( $P<0.05$ )  $6.7 \pm 2.0$  mV and increased the fractional resistance of the serosal membrane. The transference number for  $\text{HCO}_3^-$ , calculated from the voltage changes is 0.14. The fractional resistance of the serosal membrane ( $f_r^s$ ) increased significantly ( $P<0.05$ ) from  $0.14 \pm .01$  to  $0.21 \pm .02$  when luminal bath  $[\text{HCO}_3^-]$  was lowered from 50 to 0.5 mM. When serosal bath  $\text{HCO}_3^-$  and  $\text{CO}_2$  were completely replaced  $v_s$  was  $-44.9 \pm 2.4$  mV. In mucosa with normal villus morphology  $v_s$  was  $-67.9 \pm 3.9$  mV. The serosal membrane was also depolarized upon complete replacement of medium  $\text{HCO}_3^-$  and  $\text{CO}_2$  when bath pH was buffered to 7.4 with phosphate. DNDS and acetazolamide reduced by one-half the depolarization of the serosal membrane caused by lowered medium  $[\text{HCO}_3^-]$ . Replacement of serosal  $\text{Na}^+$  reduced  $v_s$   $35.8 \pm 4.0$  mV without changing  $f_r^s$ . In the presence of DNDS this response was reduced to  $5.9 \pm 3.5$ . It is concluded that a  $\text{Na}^+$ -dependent, stilbene-sensitive  $\text{HCO}_3^-$  flux resides in the basolateral membrane of the intestinal cells in parallel with a conductive  $\text{HCO}_3^-$  flux. Supported by NIDDK 26872.



**Th-AM-F7 COUPLED MULTIPLE CONVECTIVE STREAMS: A MODEL OF RENAL TUBULAR REABSORPTION OF MOLECULAR WEIGHT INDICATORS**, by Neil V. Rau and Charles J. Lumsden, Membrane Biology Group, Department of Medicine, University of Toronto, Toronto, Ontario, Canada M5S 1A8.

Secretion and reabsorption in the nephron involve the exchange of molecules across the epithelia of the renal tubule. Of particular interest is the proximal tubular exchange of molecules between the blood, cellular and tubular spaces of the kidney. The multiple indicator dilution (MID) experiment provides a means by which radiolabelled tracers are used to quantify the kinetics of molecular exchange between these spaces.

A mathematical model of this MID tracer exchange is developed to characterize the exchange of tracers as a function of unidirectional steady state flux coefficients. This model extends previous models of renal MID by treating explicitly the convective motion of both the blood and urine. The kinetic description provided by three partial differential equations is transformed to Laplace space, resulting in a system of ordinary differential equations which are solved in the transformed co-ordinates. Analytical inversions of the Laplace space solutions are performed for various limiting cases of the model, while a general solution is obtained using numerical inversion techniques. Renal MID data (blood and urine) are transformed to Laplace coordinates and compared to the Laplace transform of the model solutions to provide a least-squares estimate of the tubular transport function. Such parameter estimation forms the basis for the assessment of tubular disorders from a functional, as opposed to a morphological, approach.

**Th-AM-F8 ACTIVATION AND ANION PERMEABILITY OF A CHLORIDE CHANNEL FROM HUMAN NASAL EPITHELIA.**

Marek Duszyk, Andrew S. French and S.F. Paul Man, Departments of Physiology and Medicine, University of Alberta, Edmonton, Alberta, Canada T6G 2H7.

An important pulmonary defense mechanism is the mucociliary apparatus, which removes inhaled particles from the airways. The operation of this system is dependent on mucus fluid and ciliary activities. The quantity and composition of the fluid is controlled, in part, by the flow of ions through the airway epithelium. Transepithelial ion fluxes are produced by a net secretory flux of chloride from submucosa to mucosa and a net absorptive flux of sodium in the opposite direction. In the present studies we used the single channel patch-clamp technique to characterize anion channels in apical membranes of human nasal epithelial cells maintained in primary culture. Seals were obtained on isolated cells or on cells at the edges of confluent sheets. Single channels were studied in the excised inside-out configuration. The channel seen most often had a conductance of 18-22 pS. It did not rectify in symmetric chloride solutions, and there was no evidence of  $\text{Ca}^{++}$  activation. The anion selectivity sequence was  $\text{NO}_3^- > \text{Cl}^- > \text{HCO}_3^-$ , and the channel could be blocked completely by gluconate ions. In the inside-out configuration, the channel could be activated by the catalytic subunit (C subunit) of cAMP-dependent protein kinase and ATP. The dependence of channel conductance on chloride concentration was compared with the predictions of continuum theory and rate theory. Supported by the Canadian Medical Research Council and the Alberta Heritage Foundation for Medical Research.

**Th-AM-F9 INDIRECT ALTERATION OF THE  $\text{Ca}^{++}$ -SENSITIVITY OF A  $\text{K}^+$  CHANNEL IN TWO SV40-TRANSFORMED RENAL CELL LINES.** J Teulon, P Ronco, M Geniteau, B Baudouin, P Verroust, R Cassingena and A Vandewalle, INSERM U.192, U.64, U.246 and CNRS ER 276 Paris, France. (Introduced by SR Thomas).

Using patch-clamp techniques, we investigated the properties of ionic channels in two transformed cell lines, RCSV1 and RCSV2, with properties of proximal and distal nephron, respectively. They were established by infection of primary cultured cells (PC) from rabbit kidney cortex with the wild type SV40 virus, and grown in serum-free, hormonally defined medium. Single-channel unit currents were recorded from inside-out and outside-out membrane patches of PC, RCSV1, and RCSV2 cells. We mainly analyzed the properties of a  $\text{Ca}^{++}$ - and voltage-activated  $\text{K}^+$  channel: In PC, RCSV1 and RCSV2 cells, this channel has comparable conductances (172±13 pS, n=9; 167±9 pS, n=8 and 166±18 pS, n=5 respectively), together with a high permselectivity of  $\text{K}^+$  over  $\text{Na}^+$  ( $P_{\text{Na}^+}/P_{\text{K}^+} = 0.03$ ); it is activated by depolarization and inhibited by external TEA, internal  $\text{Ba}^{++}$ , and quinine. It is sensitive to internal calcium ( $[\text{Ca}^{++}]_i$ ) in PC (n=5), RCSV1 (n=3) and RCSV2 (n=2) cells when the external calcium concentration ( $[\text{Ca}^{++}]_e$ ) is  $10^{-9}\text{M}$  (EGTA added in the patch pipette). However, with  $[\text{Ca}^{++}]_e = 10^{-5}\text{M}$  in the pipette, this  $\text{K}^+$  channel is  $\text{Ca}^{++}$ -sensitive in PC cells only, while it is totally insensitive to  $[\text{Ca}^{++}]_i$  in RCSV1 and RCSV2 cells (n=3 and n=5, respectively). These results indirectly suggest that a  $\text{Ca}^{++}$ -pathway, possibly a  $\text{Ca}^{++}$  channel, is present in the two SV40 transformed cell lines. The  $\text{K}^+$  channel would then remain active, despite low  $[\text{Ca}^{++}]_i$  (buffered by EGTA), because of  $\text{Ca}^{++}$  diffusion from the external (patch pipette) to the internal (bath solution) side of the patch membrane. Since RCSV1 and RCSV2 cells possess contrasting biochemical properties, which probably reflect a distinct origin, we hypothesize that alteration of  $\text{Ca}^{++}$ -sensitivity of the  $\text{Ca}^{++}$ - and voltage-activated  $\text{K}^+$  channel is a characteristic feature of SV40-infected cells and may play a role in the transformation process.

**Th-AM-F10** CYTOSOLIC  $Mg^{2+}$  MODULATES WHOLE CELL  $K^+$  AND  $Cl^-$  CURRENTS IN CORTICAL THICK ASCENDING LIMB (TAL) CELLS OF RABBIT KIDNEY. Ellie Kelepouris. Dept. of Medicine, Univ. of Penn, Philadelphia, PA.

Cytosolic magnesium ( $[Mg^{2+}]_i$ ) may regulate cell function by modulating ion channels and transport mechanisms in renal tubular cells. The TAL is the major site of  $Mg^{2+}$  transport and a segment in which a significant portion of ATP utilization is devoted to NaCl transport. The role of  $[Mg^{2+}]_i$  was examined in cortical TAL cells from rabbit kidney established in long-term culture by transformation with a non-replicating SV-40 virus. The cells were studied using the whole-cell patch-clamp technique. Internal solutions contained KCl 120 mM, EGTA 10 mM,  $CaCl_2$  100 nM and varying amounts of MgATP and  $MgCl_2$  to produce free  $[Mg^{2+}]_i$  of 1 and 9.4 mM with constant (2 mM) ATP levels. Control cells dialyzed with 1 mM  $[Mg^{2+}]_i$  exhibited a linear current with a zero net current at  $-43 \pm 6$  mV ( $n=13$ ).  $Ba^{2+}$  (5 mM) inhibited 50% of outward current and shifted the zero net current toward zero  $-10 \pm 10$  mV ( $n=3$ ). The  $Ba^{2+}$  sensitive component had a reversal potential close to  $E_K$ . Bumetanide (200  $\mu$ M), on the other hand, resulted in a shift to  $-75 \pm 8$  mV ( $n=3$ ). Internal 9.4 mM  $[Mg^{2+}]_i$  markedly inhibited whole cell currents and shifted net zero current to  $-106 \pm 10$  mV ( $n=6$ ,  $p<0.05$ ). The data demonstrate the existence of  $K^+$  and  $Cl^-$  channels in these cells which retain their original transport characteristics. High  $[Mg^{2+}]_i$  suppressed both the  $K^+$  and  $Cl^-$  currents and markedly hyperpolarized the cell interior. The data therefore suggest that increasing  $[Mg^{2+}]_i$  modulates ion transport in the TAL by functioning as an internal  $K^+$  and/or  $Cl^-$  channel blocker. As  $[Mg^{2+}]_i$  is expected to rise significantly during ischemia, this may represent an endogenous mechanism to protect against ATP depletion.

**Th-AM-F11** POTASSIUM DEPENDENCE OF THE BASOLATERAL CHLORIDE UPTAKE MECHANISM IN PRIMARY CULTURES OF CANINE TRACHEAL EPITHELIUM. P. Fong and J.H. Widdicombe. Dept. of Physiology and Cardiovascular Research Institute, University of California, San Francisco, CA 94143.

Monolayer cultures of dog tracheal epithelium were pretreated with amiloride ( $10^{-4}$  M) and isoproterenol ( $10^{-5}$  M), and changes in short-circuit current ( $I_{sc}$ ) elicited by the basolateral application of  $Ba^{++}$  were monitored. A dose-dependent inhibition was observed. Eadie-Hofstee plots of data from cumulative dose-response curves revealed two inhibitory constants of  $2 \times 10^{-6}$  M and  $1 \times 10^{-4}$  M, and a maximal inhibition of  $I_{sc}$  by  $Ba^{++}$  of  $82.8 \pm 4.2\%$  (mean  $\pm$  SEM,  $n=5$ ). This value is not significantly different from the fraction of the basolateral current carried by the K conductance (5/6) with a Na/K/2Cl cotransporter, but is significantly greater than that expected for NaCl cotransport (2/3). Measurements of  $^{86}Rb$  uptake on paired tissues showed negligible influx of tracer from the apical side ( $16 \pm 2$  pEq. $cm^{-2}.min^{-1}$ ) compared to a basolateral influx of  $720 \pm 80$  pEq. $cm^{-2}.min^{-1}$  (means  $\pm$  SEM,  $n=4$ ). Basolateral influx of  $^{86}Rb$  was investigated further. Bumetanide ( $10^{-4}$  M) inhibited the initial rate of tracer uptake by  $\sim 50\%$ . Tracer influx was decreased by a similar fraction upon the substitution of Cl in the uptake medium by isethionate. The replacement of Na by N-methyl-D-glucamine reduced influx by 93%. Application of bumetanide in Na- or Cl- free medium did not further decrease  $^{86}Rb$  influx. Our data support the presence of a Na/K/2Cl basolateral cotransporter.

#### **Th-AM-F12 REGULATION OF CHLORIDE CONTENT IN SUBMUCOSAL GLAND CELLS**

Terry M Dwyer. Department of Physiology and Biophysics. University of Mississippi Medical Center. Jackson, MS. 39216-4505.

Submucosal gland cells were isolated from the surface epithelium of weanling swine trachea by digestion in collagenase and DNAase. Individual cells and small clumps of cells were plated onto coverslips coated with cell-tac, grown in medium 199 and stored in 5%  $CO_2$  at 37°. Most experiments were performed within 4 to 48 hours on these cells; additional experiments were done at 3-7 days on cells that migrated from these explants and that had grown to confluence. The general protocol was to expose the cells to SPQ [6-methoxy-N-(3-sulfo-propyl) quinolinium] for 20 min, and examine them on the stage of an Olympus IMT-2 inverted microscope, epilluminated with light from a Delta-Scan light source. Fluorescence excited at 350 nm maintained a steady intensity of emitted light at 450 nm, which was quenched by increasing the cell Cl concentration.

Step increases in fluorescence followed ionic substitutions where decreases in external Cl were accompanied by increases in K such that the Gibbs-Donnan equilibrium was maintained. Transient increases in fluorescence followed changes to a low Cl solution where the  $[K][Cl]$  product decreased. Change to a hyperosmotic solution gave a transient decrease in fluorescence; the magnitude of the decrease declined upon repeated exposures. Return to normal osmotic pressure resulted in an increase in fluorescence above baseline. Decreasing the solution's osmotic pressure resulted in a fall in fluorescence; return to normal gave a transient increase in fluorescence.

These responses were quantitatively smaller or not apparent in cells grown to confluence.

(Supported by grants from NIH, HL11678 & DA05094, and Cystic Fibrosis Foundation, G155.)